IEEE TRANSACTIONS ON ROBOTICS

On Optimal Pursuit Trajectories for Visibility-Based Target-Tracking Game

Rui Zou and Sourabh Bhattacharya D, Member, IEEE

Abstract—In this paper, we address a class of visibility-based pursuit-evasion game in which a mobile observer tries to maintain a line-of-sight (LOS) with a mobile target in an environment containing obstacles. The observer knows the current position of the target as long as the target is in the observer's LOS. At first, we address this problem in an environment containing a single corner. We formulate the game as an optimal control problem of maximizing the time for which the observer can keep the reachability set of the target in its field-of-view. Using Pontryagin's principle, we show that the primitives for optimal motion of the observer are straight lines (ST) and spiral-like curves (C). Next, we present the synthesis of the optimal trajectories from any given initial position of the observer. We show that the optimal path of the observer belongs to the class $\{ST, C - ST, ST - C - ST\}$. Given any initial position of the target, we present a partition of the workspace around a corner based on the optimal control policy of the observer.

Index Terms—Optimal control, pursuit evasion, target tracking.

I. INTRODUCTION

OBILE robots have been extensively deployed for visual surveillance in a wide range of applications, for example, search operations [1], sports coverage [2], crowd and social movement monitoring [3], [4], and wildlife research [5]. A problem that often arises in such scenarios is to keep mobile entities of interest (called *targets*) in the sensing range of the robots (called *observers*). Target tracking refers to the problem of planning motion for a mobile observer that tries to track a mobile target in the presence of obstacles. Surveillance in such surreptitious manner often involves a lack of information about the future actions of the targets. In such cases, it is often assumed that the targets either move randomly [6], [7] or they are adversarial in nature [8], [9]. In this paper, we follow the latter approach to design optimal pursuit trajectories for an observer that tracks a mobile target.

In a game-theoretic setting, several solution concepts can be used to compute the optimal strategy of a player. The

Manuscript received January 31, 2018; revised August 10, 2018; accepted November 16, 2018. This paper was recommended for publication by Associate Editor A. Ude and Editor T. Murphey upon evaluation of the reviewers' comments. This work was supported by the NSF Grant IIS-1816343. (Corresponding author: Sourabh Bhattacharya.)

- R. Zou is with The Mathworks, Inc., Natick, MA 01760 USA (e-mail: rzou@iastate.edu).
- S. Bhattacharya is with the Department of Computer Science and the Department of Mechanical Engineering, Iowa State University, Ames, IA 50011 USA (e-mail: sbhattac@iastate.edu).
- Color versions of one or more of the figures in this paper are available online at http://ieeexplore.ieee.org.

Digital Object Identifier 10.1109/TRO.2018.2882747

most common solution concept is that of a Nash equilibrium in noncooperative scenarios. For example, Bhattacharya and Hutchinson [9] use the concept of a saddle-point equilibrium to determine the optimal policy of the player in a visibility-based target-tracking game. In this paper, we use the concept of *dominant strategy* to design the controller for the observer [10]. A strategy is dominant if it earns a player a larger payoff than any of its other strategies, regardless of the actions of other players. Existence of a dominant strategy for the observer reduces the game between the observer and the target to an optimal control problem. The geometry of the sensing model of the observer around a corner, and the reachability set of the target permits a dominant strategy for the observer. The dominant strategy can be implemented in an open-loop manner, and provides local guarantees on the tracking performance.

The contributions of this paper are as follows. For the targettracking problem around a corner, we use the concept of dominant strategy to derive the optimal control of the observer in the class of open-loop strategies. We show that the motion primitives for optimal tracking are straight line (ST) and spiral-like curves (C) around the corner. Using the primitives, we synthesize the optimal trajectory of the observer, and show that they belong to the class $\{ST, C - ST, ST - C - ST\}$. We present a cell decomposition of the workspace around the corner based on the nature of the optimal trajectory. The framework proposed in this paper is general, and can be used to characterize the optimal policy of the agents with complex dynamics. Additionally, the control policy for the observer does not require knowledge about the instantaneous velocity of the target, which is a significant improvement compared to the policies previously proposed in [11] from an implementation perspective.

The rest of this paper is organized as follows. In Section II, we present a review of the literature related to the tracking problem. In Section III, we present the formulation of the target-tracking problem around a single corner. In Section IV, we obtain the motion primitives for the observer based on Pontryagin's minimum principle. In Section V, we present the synthesis of the optimal trajectories. In Section VI, we present a cell decomposition of the workspace around a corner based on the optimal strategy of the observer. In Section VII, we present our conclusions and future research directions.

II. RELATED WORK

The problem of target following was initially introduced in [12]. The authors proposed motion planning algorithms for a

robot to maintain visibility with a target in a cluttered environment. A numerical solution is proposed for a predictable target. However, no guarantees for tracking can be obtained for an unpredictable target. In case of a cooperative target, formation control techniques [13] as well as model-predictive control [14], [15] techniques have been proposed to plan the path of the observer. For a randomly moving target, there is an extensive literature on designing observer's trajectory that minimizes the uncertainty in the predicted location of a target [7], [16]. Although it might be reasonable in some practical scenarios to assume a random walk model for an unpredictable target [17], considering worst case behavior of a target provides robust tracking strategies [18].

In the past, robust techniques for tracking unpredictable targets have been proposed based on worst case analysis. This naturally lends to a game-theoretic framework [19] in which the target is assumed to be adversarial in nature. Moreover, since a pursuit-evasion game ensues between the observer and target, the theory of differential games [20] can be used to obtain the optimal strategy for the observer. In a game, the optimal policy of the observer depends on its set of allowable strategies and information regarding the target [21]. For an observer that has information regarding the current velocity of the target, Bhattacharya and Hutchinson [11] solve the problem of maximizing the time for which the target can remain within the sensing footprint of the observer around a corner. The result around the corner is extended to provide bounds on the initial position of the observer from which it can track in general environments. In the class of position-based feedback strategies, Bhattacharya and Hutchinson [9] provide structural properties of the optimal trajectories for the observer in general environments, which are used to compute the optimal trajectory of the observer in simple environments [22], [23]. In summary, efforts in this direction have primarily led to insights into the structural properties of optimal trajectories for the observer in general environments [11], [24] which in turn have been used to construct optimal trajectories for the observer in simple environments [22]. However, their extension to general environments containing multiple obstacles has been rather limited.

In this paper, we use the framework of optimal control theory to obtain the observer's motion. Optimal control theory has been extensively applied in motion planning of mobile robots. Minimal length paths and time-optimal trajectories have been obtained for robots with different dynamic and kinematic configurations. For example, in [25], the time optimal trajectories for differential drive robots (DDRs) with bounded velocity are presented. The primitives of minimum wheel-rotation paths for DDRs are presented in [26]. Optimal paths and velocity profiles for carlike robots that minimize the energy consumption is presented in [27]. Many applications relevant to target-tracking/pursuit evasion include: vision-based time-optimal strategy for a differential-drive pursuer to capture an evader [28], [29]; optimal strategy for the pursuer to maintain a constant distance with the evader at minimal velocity [30]; time-optimal primitives for a pursuit-evasion game between an omni-directional agent and a DDR in which the two agents can switch roles. However, these works are limited to an

obstacle-free environment [31]. Finding optimal trajectories for a robot to a fixed point has been proved to be a challenging problem in the presence of obstacles [32]–[34], not to mention the problem of finding the optimal tracking strategy of a pursuer in such environment. Therefore, a complete construction of optimal tracking trajectories for a robot are primarily limited to environment with simple obstacles [18], [22].

In the past, there have been some efforts to address the target-following problem with sensing constraints. In [35], Murrieta-Cid et al. address the problem of target following for an observer equipped with a sensor that has a limited range. They provide a necessary condition for tracking based on the cylindrical algebraic decomposition of the environment proposed originally by Schwartz and Sharir. In [36], the framework of chance-constrained optimization [37] is used to propose a onestep look-ahead motion strategy that maximizes the probability for keeping the target in the sensing footprint of an observer with a limited field-of-view (FOV). The presence of obstacles imposes constraints in sensing in addition to the constraints on the positions of both the observer and the target. This gives rise to optimization problems with joint state and control constraints also referred to as mixed constraints. The presence of such constraints has long been known to constitute a challenge as regards the derivation of appropriate necessary conditions of maximum principle type. Problems with mixed constraints have been studied systematically by Hestenes [38], Gamkrelidze [39], and Neustadt [40] among many others, and remain an active subject [41]-[48]. The necessary conditions for optimal control problems with mixed constraints can be characterized as the optimal solutions of multipoint boundary value problems (MBVP). The solutions of the MBVP can be numerically computed using shooting techniques [49], [50] and direct methods [51]–[53]. In this paper, we use a different approach to deal with the mixed constraints. We lift the problem into space-time coordinates which in turn converts the dynamic optimization problem into a static one. The mixed constraints either appear as boundary conditions or as constraints on the curvature of the optimal trajectories.

III. PROBLEM STATEMENT

In this section, we present the formulation of the target-tracking problem studied in this paper. Consider a planar environment containing multiple polygonal obstacles. Two mobile agents, an observer and a target, are present on the plane. We assume that they all have an omni-directional FOV with infinite range. They are visible to each other when the line joining them [line-of-sight (LOS)] does not intersect with the obstacle. We assume that the target is initially visible to the observer. The observer's objective is to maintain an LOS with the target for the maximum possible time, whereas the target's objective is to break LOS in the minimum time. Based on the above-described formulation, we address the following problem: what should be the optimal strategy for the observer to maximize the time for which it can maintain an LOS with the target without any information about the target's strategy?

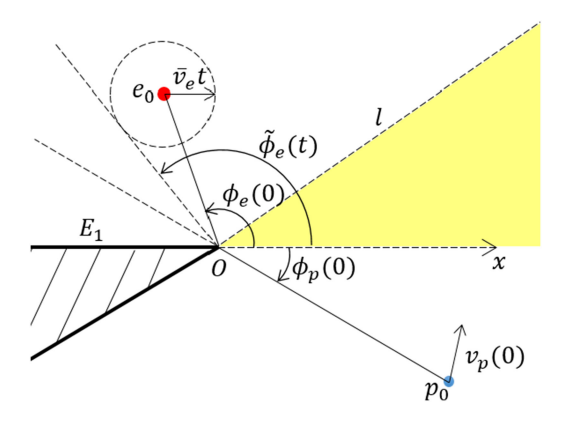


Fig. 1. Illustration of optimal control problem.

In this paper, we address the problem around a corner. In order to account for the worst case scenario, we assume an adversarial target that tries to break the LOS in minimum amount of time. Since the two agents in the problem have exactly opposite objectives in this formulation, and they are mobile, a pursuit-evasion game arises. Hereafter, we use the term pursuer interchangeably with observer, and evader interchangeably with the target. Both agents are assumed to be holonomic.

Consider a planar environment containing a semi-infinite obstacle having one corner, as shown in Fig. 1 (dashed area). Let the vertex be the origin, and let edge E_1 represent the negative x-axis. Let $\mathcal{C} = \mathbb{R}^2$ be the configuration space. Let $\mathcal{C}_{\text{obs}} \subset \mathcal{C}$ be the obstacle region. Thus, the free configuration space is defined as $C_{\text{free}} = C \setminus C_{\text{obs}}$. Two mobile agents: one pursuer and one evader move on the plane with velocities $v_p(t)$ and $v_e(t)$, respectively. Their speeds are upper bounded by \bar{v}_p and \bar{v}_e , respectively. Let $a=\bar{v}_e/\bar{v}_p$ denote the ratio of the maximum speeds of the two agents. Their positions p(t) and e(t) are denoted by $(x_p(t), y_p(t))$ and $(x_e(t), y_e(t))$ in Cartesian coordinates and $(\phi_p(t), r_p(t))$ and $(\phi_e(t), r_e(t))$ in polar coordinates, respectively. Let $p_0 = p(0)$, $e_0 = e(0)$ and $d_p(t) = |y_p(t)|$, $d_e(t) = |y_e(t)|$. Let $d(x, S) = \inf_{y \in S} ||x - y||_2$ denote the infimum distance of a point x to a set S which may be a ray, a line or a region. V(x) denotes the visibility polygon [54] of a point $x. S^*$ denotes the star region that is defined as the region opposite to the obstacle across the vertex bounded by line l and the positive x-axis shown as the yellow region.

If $p(t) \in S^*$, the pursuer can track the evader forever, since the entire free space $\mathcal{C}_{\text{free}}$ is visible to it. The evader can win the game in the following ways: first, the evader can break the LOS with the pursuer around the corner. (When LOS is broken at a time t_f , their positions p_f and e_f are collinear with O, and the angular speed of the evader around the corner is greater than the angular speed of the pursuer around the corner). Second, the evader can reach the origin before the pursuer reaches the star region associated with the vertex. In this case, the evader can win by moving along the edge of the obstacle that is not visible to the pursuer.

IV. MOTION PRIMITIVES FOR THE OBSERVER

In this section, we derive the primitives for the pursuer's trajectory. First, we introduce the concept of a dominant strategy

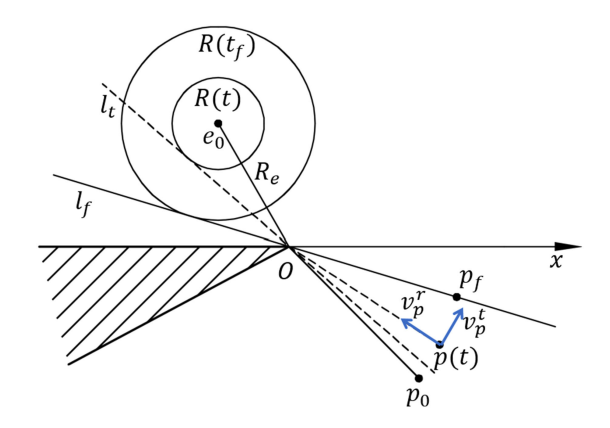


Fig. 2. Tracking environment around a corner.

for the pursuer, and discuss its relevance to the problem. In a game-theoretic setting involving multiple players, a strategy is dominant if it earns a player a larger payoff than any of its other strategies, regardless of the actions of other players. Hence, a strategy is dominant if it is always better than any other strategy, for any profile of other players' actions. Since the evader is unpredictable, the pursuer lacks knowledge about the future control policy and trajectory of the evader. However, at any time t, the evader is located inside its reachable set, denoted as R(t). A strategy for the pursuer that keeps $R(t') \subset V(p(t')) \forall t' \leq t$ succeeds in tracking the evader for time t. Additionally, such a strategy is dominant since it keeps the evader within the pursuer's FOV irrespective of the evader's strategy until time t. Therefore, we formulate the problem of persistent tracking for an unpredictable evader as a problem of computing a dominant strategy for the pursuer which ensures $R(t) \subset V(p(t))$. This gives rise to the following problems.

- 1) An optimal control problem: In case the pursuer has no strategy to reach the star region while maintaining the visibility of the evader, we compute a strategy to maximize the time for which it can ensure $R(t) \subset V(p(t))$.
- 2) A reachability problem: In case the pursuer can reach the star region using several strategies while maintaining the visibility of the evader, we compute one of them. Once the pursuer reaches the star region, it can see the evader forever. An important thing to note here is that the previous statement is not true in environments containing multiple corners. However, the computation of a strategy is required for the sake of completeness of the solution to the persistent tracking problem around a single corner.

We assume that p(0) lies in the fourth quadrant, and e(0) lies in the second quadrant (refer to Fig. 2). In Section VI-A, we relax this assumption, and solve the problem for arbitrary position of the pursuer and evader. In our case, R(t) is a disc of radius $\bar{v}_e t$ centered at e_0 . For an evader with higher order dynamics or motion constraints, analytical [55]–[59] as well as numerical [60] tools are available to compute the reachable sets. l_t is the tangent to R(t) passing through O. As the radius of R(t) increases, l_t rotates counterclockwise. In order to keep R(t) within its FOV, p(t) should lie above or on l_t . The game terminates at the moment when the pursuer lies on l_t , and does not have enough tangential velocity to "keep up" with l_t . We can

imagine the pursuer to be a kinematic agent moving on the plane trying to avoid getting hit by a rotating bar (l_t) . The termination condition can be mathematically expressed as follows:

$$\tilde{\phi}_e(t) - \phi_p(t) = \pi, \quad \frac{\bar{v}_e}{\sqrt{(R_e^2 - \bar{v}_e^2 t^2)}} > \frac{\bar{v}_p}{r_p(t)}$$
 (1)

where $R_e = r_e(0)$. The second condition in (1) refers to the condition that the angular velocity of l_t is greater than the angular velocity of the pursuer around O. If the game does not terminate, then the pursuer is capable of staying above l_t until it reaches the star region. Therefore, the geometry of the problem around the corner allows us to find the maximum time for which a dominant strategy exists for the pursuer.

Let $x_1(t)$, $x_2(t)$, and $x_3(t)$ denote the states that represent $\tilde{\phi}_e(t)$, $r_p(t)$, and $\phi_p(t)$, respectively. Let $\mathbf{u} = \{u_1, u_2\} \in \mathbb{S}^1 \times \mathbb{R}^+$ denote the control input, where $u_1(t)$ is the angle between the pursuer's velocity and its tangential direction with respect to the radial line from the origin, and $u_2(t) = |v_p(t)|$ is the magnitude of $v_p(t)$. From the equations of motion, we obtain the following state equations:

$$\dot{x}_1 = \frac{\bar{v}_e}{\sqrt{R_e^2 - (\bar{v}_e t)^2}}, \quad x_1(0) = \phi_e(0)$$
 (2)

$$\dot{x}_2 = -u_2 \sin u_1, \qquad x_2(0) = R_p \tag{3}$$

$$\dot{x}_3 = \frac{u_2}{x_2} \cos u_1, \qquad x_3(0) = \phi_p(0)$$
 (4)

where \dot{x}_1 describes the motion of l_t as the disc's radius increases at a rate of \bar{v}_e , \dot{x}_2 describes the pursuer's motion in radial direction, and \dot{x}_3 describes the pursuer's motion in tangential direction. Let the dynamics of the system be represented as $\dot{\mathbf{x}}(t) = f(\mathbf{x}, \mathbf{u}, t)$ where $\mathbf{x} = \{x_1, x_2, x_3\}$ and $\mathbf{u} = \{u_1, u_2\}$ represent the state and control vector, respectively.

The objective of the pursuer is to minimize the performance index

$$J = \int_0^{t_f} -1dt \tag{5}$$

where t_f denotes the first time at which the termination conditions (1) are satisfied. In terms of the states, the terminal conditions are as follows:

$$g_1(\mathbf{x}(t_f), t_f) = x_1(t_f) - x_3(t_f) - \pi = 0$$

$$g_2(\mathbf{x}(t_f), t_f) = \dot{x}_1(t_f) - \dot{x}_3(t_f)$$
(6)

$$= \frac{\bar{v}_e}{\sqrt{R_e^2 - (\bar{v}_e t_f)^2}} - \frac{u_2(t_f)}{x_2(t_f)} \cos u_1(t_f) > 0.$$

In order to maintain visibility before termination, the following state inequality constraint must be satisfied:

$$S(\mathbf{x}(t)) = \pi - x_1(t) + x_3(t) > 0.$$
 (8)

Equation (8) is a first-order state inequality constraint [61] with the following derivative with respect to time:

$$S^{(1)}(t) = \frac{u_2(t)}{x_2(t)} \cos u_1(t) - \frac{\bar{v}_e}{\sqrt{R_e^2 - (\bar{v}_e t)^2}}.$$
 (9)

The Hamiltonian for the constrained system is defined as follows:

$$H(\mathbf{x}(t), \mathbf{u}(t), \mathbf{p}(t), \mu(t), t) = -1 + \mathbf{p}^{T} f + \mu S^{(1)}$$

$$= -1 + (p_{1} - \mu) \frac{\bar{v}_{e}}{\sqrt{R_{e}^{2} - (\bar{v}_{e}t)^{2}}}$$

$$+ u_{2} \left(-p_{2} \sin u_{1} + \frac{p_{3} + \mu}{x_{2}} \cos u_{1}\right) + \mu S^{(1)}$$
(10)

where $\mathbf{p} = \{p_1, p_2, p_3\}$ are costates, and $\mu(t) \geq 0$ is the influence function defined as follows:

$$\mu = \begin{cases} 0 & S > 0, \text{ boundary constraint inactive} \\ > 0 & S = 0, S^{(1)} = 0, \text{ boundary constraint active} \end{cases}$$
(11)

Using Pontryagin's minimum principle, the optimal control of the pursuer is given by the following equation:

$$(u_1^*, u_2^*) = \arg\min_{u_1, u_2} H(\mathbf{x}(t), \mathbf{u}(t), \mathbf{p}(t), \mu(t), t).$$
 (12)

In the rest of this paper, * is used to denote quantities associated with optimal solution to (5).

A. Inactive Boundary Constraints

Using Pontryagin's minimum principle, we can show that the pursuer moves on a straight line (ST) path with speed \bar{v}_p when the boundary constraint is inactive (i.e., $\mu=0$). The proof is presented in the Appendix. Additionally, the following property holds at termination.

Proposition 1: The pursuer's velocity is always orthogonal to the bar at termination.

Proof: Please refer to the proof in the Appendix.

In [62], we analyzed the target-tracking problem for an observer that tries to track a mobile target for a finite time T around a corner. The analysis presented in [62] only considered the case when the boundary constraints are inactive. Since the necessary conditions for optimality do not depend on the duration for which the game is played, it leads to the same result when the boundary conditions are inactive. The remaining sections in this paper investigate the optimal trajectory of the pursuer for the case when the boundary constraints are active, which is not considered in [62]. Therefore, a complete solution to the optimal control problem for the pursuer around the corner is presented in this paper.

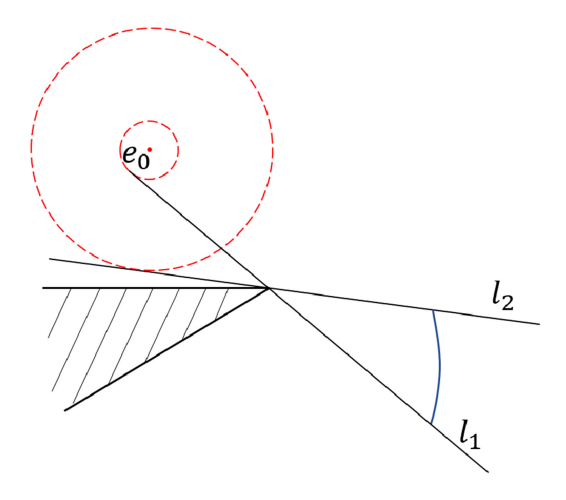
B. Active Boundary Constraints

In this section, we will address the case in which the boundary constraints are active. When the boundary constraint is active, the pursuer's trajectory satisfies the following equations:

$$S(\mathbf{x}(t)) = \pi - x_1(t) + x_3(t) = 0$$

$$S^{(1)}(t) = \frac{u_2(t)}{x_2(t)} \cos u_1(t) - \frac{\bar{v}_e}{\sqrt{R_e^2 - (\bar{v}_e t)^2}} = 0.$$

The above-mentioned equations model the fact that the pursuer is collinear with l_t and rotates with it at the same angular speed.



"Spiral" (C) trajectory of the pursuer when it rotates along with l_1 at speed \bar{v}_p and stops at l_2 .

In other words, the pursuer "stays" on the rotating bar representing l_t . The angular speed of the rotating bar at any time is given by $\omega(t) = \bar{v}_e / \sqrt{R_e^2 - \bar{v}_e^2 t^2}$ which is also the angular speed of the pursuer when the boundary constraints are active. The pursuer moves with its maximum speed \bar{v}_p at all times. Let $v_n^t(t)$ and $v_n^r(t)$ represent the pursuer's velocity in the tangential and radial direction, respectively. We obtain the following expressions for $v_n^t(t)$ and $v_n^r(t)$:

$$v_{p}^{t}(t) = \frac{\bar{v}_{e} \cdot r_{p}(t)}{\sqrt{R_{e}^{2} - (\bar{v}_{e}t)^{2}}}, \quad v_{p}^{r}(t) = \sqrt{\bar{v}_{p}^{2} - [v_{p}^{t}(t)]^{2}}$$

$$\Rightarrow \dot{\phi}_{p} = \frac{\bar{v}_{e}}{\sqrt{R_{e}^{2} - \bar{v}_{e}^{2}t^{2}}}, \quad \dot{r}_{p} = \sqrt{\bar{v}_{p}^{2} - \omega^{2}t^{2}}.$$
(14)

$$\Rightarrow \dot{\phi}_p = \frac{\bar{v}_e}{\sqrt{R_e^2 - \bar{v}_e^2 t^2}}, \quad \dot{r}_p = \sqrt{\bar{v}_p^2 - \omega^2 t^2}. \tag{14}$$

Note that counterclockwise and toward the origin are defined as the positive directions of the pursuer's tangential and radial velocities, respectively. Fig. 3 shows a trajectory of the pursuer from its initial position when the boundary constraints are active. The blue curve represents the pursuer's trajectory when it rotates with the bar from line l_1 to l_2 . Termination occurs when $v_n^t(t) = \bar{v}_p$, since the bar keeps increasing its angular speed while the pursuer can no longer do so as it cannot reduce its radius or increase its tangential speed. We use the term "spiral" to refer to the pursuer's trajectory when the boundary constraints are active.

From the necessary conditions of optimal trajectories, we can conclude that the optimal trajectory of the pursuer is comprised of only straight line segments ("ST") and spirals ("C").

V. SYNTHESIS OF OPTIMAL TRAJECTORIES

From the previous section, we can conclude that the optimal trajectory for the pursuer is a concatenation of ST and C. In this section, we present the synthesis of the optimal trajectories. The trajectories are optimal in the following sense. Given an initial position of the pursuer, the trajectories maximize the time for which the pursuer can keep the reachability set of the evader within its visibility polygon if it cannot reach the star region while ensuring $R(t) \in V(p(t))$ for all t. In case the pursuer

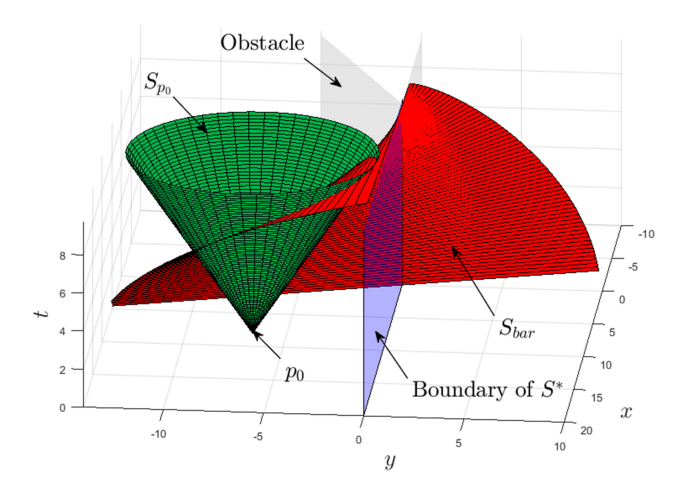


Fig. 4. Surface swept by the bar and reachable cone of the pursuer in x-y-tspace.

can reach the star region while keeping the reachable set of the evader its FOV, we present a feasible strategy for the pursuer.

A. Lifting to x-y-t Space

In this section, we present a description of the optimal control problem stated in the previous section in an extended space by augmenting time as an additional dimension to the x-y plane. To be specific, we reformulate the tracking problem in x - y t space. This converts the dynamic optimization problem of generating trajectories for the pursuer on a plane into a static optimization problem of computing maximal length paths in space-time coordinates under constraints [from the necessary conditions (12)] presented in the previous section.

Fig. 4 shows the corner and the space around it in x - y - tcoordinates. The initial positions of the players p_0 and e_0 is represented as points on the plane t = 0. As time progresses, the trajectory of the pursuer is a curve in the x - y - t space. Next, we describe the motion of the line/bar l_t in the x-y-tspace, and the reachable set of the pursuer. As the bar rotates around the origin with angular velocity $\omega(t) = \frac{\bar{v}_e}{\sqrt{R_e^2 - (v_e t)^2}}$, it forms a ruled surface in the x-y-t space (refer to Fig. 4). We denote it as S_{bar} . The bar rotates around the corner until it is aligned with a boundary of the obstacle/ S^* (x-axis) in time $T = d_e/v_e$ where d_e denotes the initial distance of e_0 from edge E_1 in Fig. 1. $R(t) \in V(p(t))$ if and only if p(t) lies between $S_{\rm bar}$ and the x-y plane. The pursuer's reachable set in the three-dimensional (3-D) space is a cone originating from its initial position. We denote it as S_{p_0} (refer to Fig. 4). At time t, the radius of the cone is $\bar{v}_p t$. The pursuer's objective is to maximize the time from being hit by a rotating bar if it cannot reach S^* .

In the previous section, we showed that optimal trajectories are comprised of C and ST. We will refer to them as primitives, since the optimal path is obtained by concatenating the primitives. Based on the aforementioned fact, a path obtained by concatenating C and ST segments is a candidate for an optimal path. Let "-" correspond to smooth transitions, and "*" correspond to non-smooth transitions between two consecutive

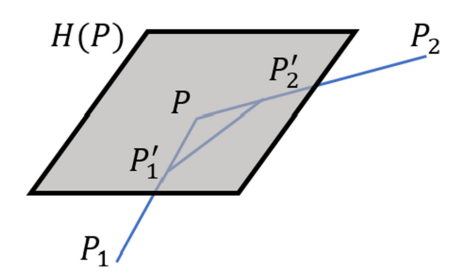


Fig. 5. Two consecutive ST segments with transition point P lying on S_{bar} .

primitives. From the previous section, we know that the pursuer moves with the maximum speed \bar{v}_p on the optimal path. Since the spirals are solution to (14), two distinct spirals never intersect (Cauchy–Lipschtiz theorem [63]). Hence, transition between two distinct C curves is not possible. The next lemma shows that non-smooth transitions between two ST segments are not possible.

Lemma 1: The optimal path cannot contain transitions of the type ST * ST.

Proof: We prove this lemma by contradiction. Consider an ST * ST path P_1P_2 , which is a part of an optimal path. We will show that we can modify P_1P_2 to generate a new path on which the pursuer can track for a longer time. First, we would like to introduce the concept of "below" and "above" in 3-D. A pursuer's position in 3-D is "below" a surface if its projection onto the surface along the t-axis has a greater t. The concept of "above" is defined similarly. It is clear that if a pursuer's position is below the red surface S_{bar} , then the pursuer is ahead of the bar. Let PP_1 and PP_2 denote the two ST line segments, as shown in Fig. 5. Since the pursuer can see the evader along P_1P_2 , both PP_1 and PP_2 are below $S_{\rm bar}$ except for point P. P lies on $S_{
m bar}$ since transition between paths can only occur when the boundary conditions are active. Since S_{bar} is differentiable at every point, it has a tangent plane at every point. Define H(P) to be the tangent plane at point P. Consider an ϵ ball around P with $\epsilon > 0$ that intersects PP_1 at P'_1 and PP_2 at P_2' . Then locally, there always exists an ϵ ball such that P_1' and P_2' are below the tangent plane H(P). Therefore, line segment $P_1'P_2'$ is below H(P), thus below S_{bar} . So the pursuer is able to move along $P_1P_1'P_2'P_2$ while maintaining visibility. Moreover, in 3-D, the pursuer takes the same time to move on $P'_1P'_2$ and PP_1P_2 , meaning it does not move at full speed \bar{v}_p on $P'_1P'_2$. So if the pursuer moves on $P'_1P'_2$ at full speed, it can reach P'_2 in a shorter time and thus track the evader for a longer time. Therefore, the tracking time on an ST * ST path (in which the transition between ST segments occurs on $S_{\rm bar}$) can be improved by replacing it with an ST * ST * ST path in which the transition between ST segments occur in free space (inactive boundary conditions). Note that the lemma makes no claims about the optimality of the new path. In fact, the ST * ST * STpath in free space cannot be optimal since only an ST segment can be optimal when the boundary conditions are inactive.

Therefore, we can conclude that the optimal path of the pursuer belongs to the family $\{ST, C, C*ST, ST*C, C-ST, \ldots, C-ST-C-\ldots, ST-C-ST-C-\ldots\}$ i.e.,

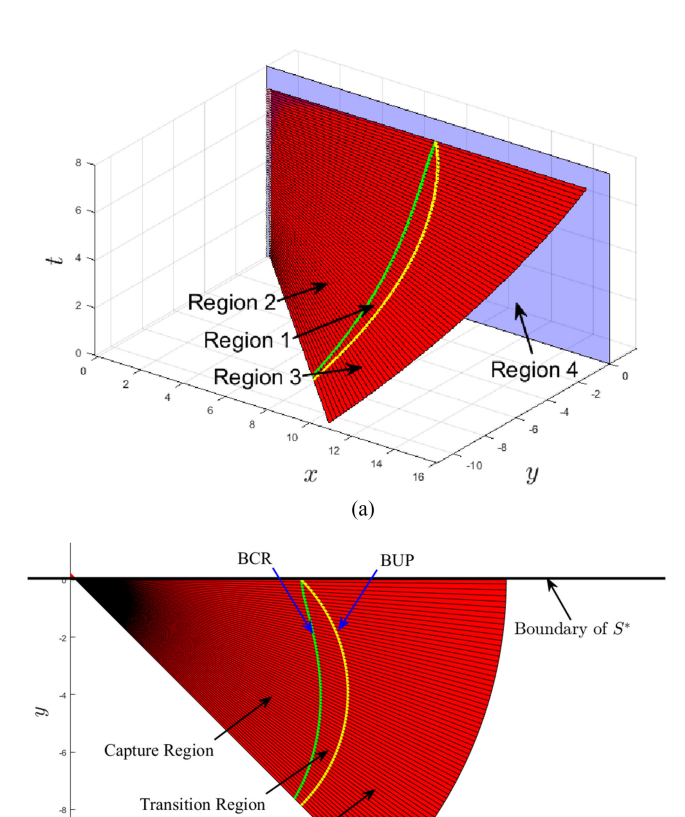


Fig. 6. (a) Terminal manifold $S_{\rm bar}$ and its partition in x-y-t space. (b) Projection of $S_{\rm bar}$ and its partition on the x-y.

(b)

Usable Part

any sequence of primitives in which two ${\cal C}$ or ${\cal ST}$ paths are not consecutive.

B. Description of the Terminal Manifold

In this section, we provide a description of the points in the x-y-t space at which either the pursuer loses sight of the evader or can see the evader forever. These are points at which the tracking game terminates, since either of the players can ensure their desired outcome.

If the pursuer reaches the boundary of the S^* [denoted as Region 4 in Fig. 6(a)] without losing sight of the evader, it can see the evader forever. Therefore, Region 4 in Fig. 6(a) denotes the set of termination points at which the pursuer can track the evader forever. If the evader breaks the LOS with the pursuer, the pursuer lies on the bar at termination. Therefore, the surface $S_{\rm bar}$ is the termination manifold for which the evader breaks the LOS with the pursuer. Additionally, termination occurs when the pursuer does not have sufficient tangential velocity to move with the bar. This occurs when the radial distance of the pursuer r_p at which it gets hit by the bar is greater than $\bar{v}_p/\omega(t)$. This is called the *Usable Part* (UP) [20] or Region 3 of the terminal manifold x-y-t space. Fig. 6 shows the UP. The yellow curve represents the boundary of the UP (BUP).

As discussed in Section III-B, the pursuer traces a spiral while moving along with the rod when the boundary constraints are active. The green curve in Fig. 6 is the spiral traced by a pursuer that moves with the bar from t=0, and reaches the point of intersection between the BUP and S^* . The region between the green curve and the BUP is called the transition region or Region 1. If the pursuer lies in the transition region, the spiral traced by moving along with the bar (active boundary constraints) terminates on the BUP. The region to the left of the green curve on S_{bar} is called the *capture region* or Region 2. If the pursuer lies in the capture region, it can follow the spiral traced by moving along with the bar (active boundary constraints) and reach the boundary of S^* , as shown in Fig. 6. The green curve is called the boundary of the capture region. Based on the above discussion, we can conclude that the trajectory of the pursuer until termination is known if it lies in Region 2 or 3. In the next section, we construct optimal trajectory for a pursuer that lies in the transition region.

C. Optimal Strategy in the Transition Region

In this section, we present the optimal strategy for a pursuer that lies in the transition region. The main result in this section is summarized in the following proposition.

Proposition 2: When the pursuer lies in the transition region, its optimal trajectory belongs to the family $\{C-ST,ST\}$. The transition from C to ST occurs at the first instant at which the pursuer can terminate the game on an ST path without losing visibility of R(t).

The outline of the proof is as follows. First, we show that if a pursuer can follow an ST path to termination, it is the optimal trajectory. However, that might not be possible from all points in the transition region due to the constraints imposed by Proposition 1 for termination on an ST path. Next, we present a partition of the transition region based on the sign of the curvature of the spirals passing through the points in the partition. We show in Lemma 5 that if the pursuer lies in the partition in which the spirals are of negative curvature, it is possible to follow an ST path that respects the constraints imposed by Proposition 1, thereby rendering the ST path optimal. Finally, we show that the optimal paths from the remaining points in the transition region belong to the category C - ST. Based on the lemmas, we present a formal proof of Proposition 2 at the end of the section.

Fig. 7(a) shows $S_{\rm bar}$ for an arbitrary initial position of the evader in the second quadrant, and S_p in the x-y-t space for an arbitrary initial position of the pursuer in the transition region. The height of the cone is equal to the time taken by the bar to reach the boundary of the star region. In Fig. 7(b), the region enclosed by the red curve is the projection of the transition region on the x-y plane. The pursuer starts from a point $p(t_1)$ in the transition region, as shown in Fig. 7, at time t_1 . The cone S_{p_1} in Fig. 7(a) shows the reachable set of the pursuer. The boundary of its intersection with $S_{\rm bar}$ is shown by the curve drawn in blue, and its projection on the x-y plane is shown by the blue curve in Fig. 7(b). Inside the blue curve, $S_{\rm bar}$ is above S_{p_1} , i.e., for any given x-y, the t-coordinate on $S_{\rm bar}$

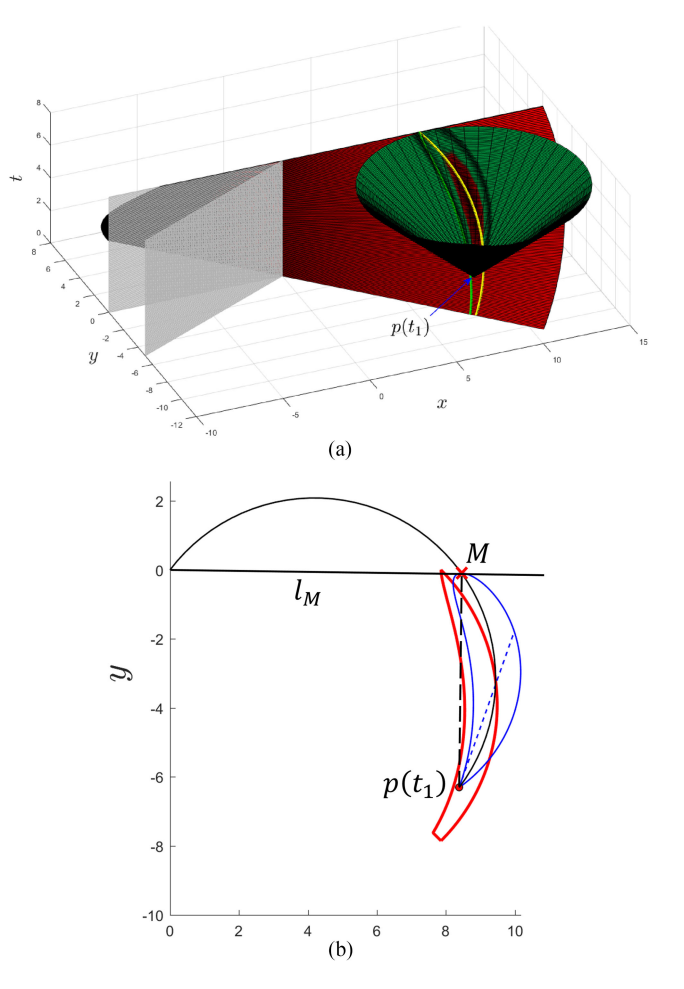


Fig. 7. (a) Intersection of the reachable set of the pursuer with $S_{\rm bar}$ in the x-y-t space when the initial position of the pursuer lies inside the transition region. (b) Projection of the intersection on the x-y plane.

is greater than the t-coordinate on S_{p_1} . Outside the blue curve, S_{p_1} lies above $S_{\rm bar}$. Since $p(t_1)$ lies in the transition region, the pursuer has enough speed to leave the bar, and move on a straight line for a while in certain directions. Subsequently, the pursuer is "caught" by the bar, and S_{p_1} and $S_{\rm bar}$ intersect at that instant. In other words, the pursuer can reach a part of the closed blue curve in Fig. 7(b) by moving on a straight line from $p(t_1)$. We call these set of points as the *admissible part* of the blue curve, and the set of ST paths that terminate on the admissible part as *feasible*. In Fig. 7(b), the part of the blue curve on the right-hand side of the dashed blue line is the admissible part.

In Fig. 7(b), M is the intersection of the blue curve and semicircle with diameter $Op(t_1)$. Since M lies on the blue curve (intersection of reachable set of the pursuer and $S_{\rm bar}$), the pursuer lies on l_M (the bar at M) if it has a straight line reaching it. Additionally, since $l_M \perp Mp(t_1)$, it is the optimal trajectory since the pursuer will take a longer time to reach l_M on any other path, thereby losing visibility of the disc before t_1 . The following lemma summarizes the above discussion.

Lemma 2: When the pursuer lies in the transition region, its optimal strategy is to move on a feasible ST until termination respecting the constraints of Proposition 1.

Next, we show the following: first, if an ST path to termination is not feasible from $p(t_1)$, then the pursuer should follow the spiral until it reaches a point from which an ST path to termination is feasible. Second, such a point exists on the spiral before the pursuer reaches the BUP on the spiral. In order to establish the aforementioned facts, we first present some structural properties of the spirals traced by the pursuer in the transition region.

Property 1: The curvature of the spirals in the transition region changes sign once in the transition region. The curvature is positive in the beginning at t=0, and negative before it terminates on the BUP. The locus of inflection points, denoted as γ_{\inf} , is given by the following curve in polar coordinates $r(t) = \frac{2\bar{v}_p}{\omega\sqrt{\omega^2t^2+4}}, \, \theta(t) = \sin^{-1}(\frac{\bar{v}_e t}{R_e}) \,$ where $\omega(t) = \frac{\bar{v}_e}{\sqrt{R_e^2 - \bar{v}_e^2t^2}}.$ Note that there is an inflection point on the bar corresponding to some spiral for every $t \in \{0, T\}$, where T denotes the time required by the bar to reach the star region. Moreover, the location of the inflection point on a bar is dependent on t and ω . We use $r_{\inf}(t)$ to denote the distance of the inflection point from the origin on the bar at time t. We use γ_{\inf} to denote the locus of inflection points.

Property 2: Fig. 8(a) shows $\gamma_{\rm inf}$ on $S_{\rm bar}$ in the transition region, and Fig. 8(b), shows its projection on the x-y plane. $\gamma_{\rm inf}$ partitions the transition region into two parts. The partition enclosed between $\gamma_{\rm inf}$ and the BUP is denoted as $\gamma_{\rm inf}^-$. The other partition is denoted as $\gamma_{\rm inf}^+$. The superscript denotes the curvature of the spiral in the partition.

Property 3: Consider two spirals C_1 and C_2 with initial conditions $(r_{10},\phi_e-\pi,0)$ and $(r_{20},\phi_e-\pi,0)$, respectively. Since two distinct spirals do not intersect, $r_1(t)>r_2(t)$ at all t. Therefore, the relative order of distance from the origin at any time is maintained along the spirals. We use the term *inner* to refer to all spirals that have smaller radial distance compared to a given spiral at the same time. Likewise, we use the term *outer* to refer to all spirals that have a larger radial distance compared to a given spiral at the same time.

Property 4: Given two pursuer positions on the same bar, the one closer to the origin has a longer tracking time.

Property 5: If a pursuer moves on feasible ST contained in γ_{\inf}^+ , it reaches an outer spiral.

The proof for Property 1 and Property 4 are given in the Appendix. Property 2 follows from Property 1. Property 3 defines the relative position of two spirals in terms of their radial distance from the origin. Property 5 arises from the fact that spirals in γ_{\inf}^+ have a positive curvature. Therefore, any feasible ST path followed by the pursuer will lead it to an outer spiral in γ_{\inf}^+ . A formal proof of Property 5 is presented in the Appendix.

From any point in the transition region, the pursuer can either follow a C or an ST. Property 4 and Property 5 imply that following an $ST \in \gamma_{\inf}^+$ reduces the tracking time. The next lemma shows that an ST path is optimal if the pursuer does not lie on γ_{\inf}^+ .

Lemma 3: If $p(t_1) \in \gamma_{\inf} \cup \gamma_{\inf}^-$, the optimal path is ST.

Proof: Consider a terminal ST segment on a pursuer's optimal path. Let the pursuer be located on a bar at time t_1 at

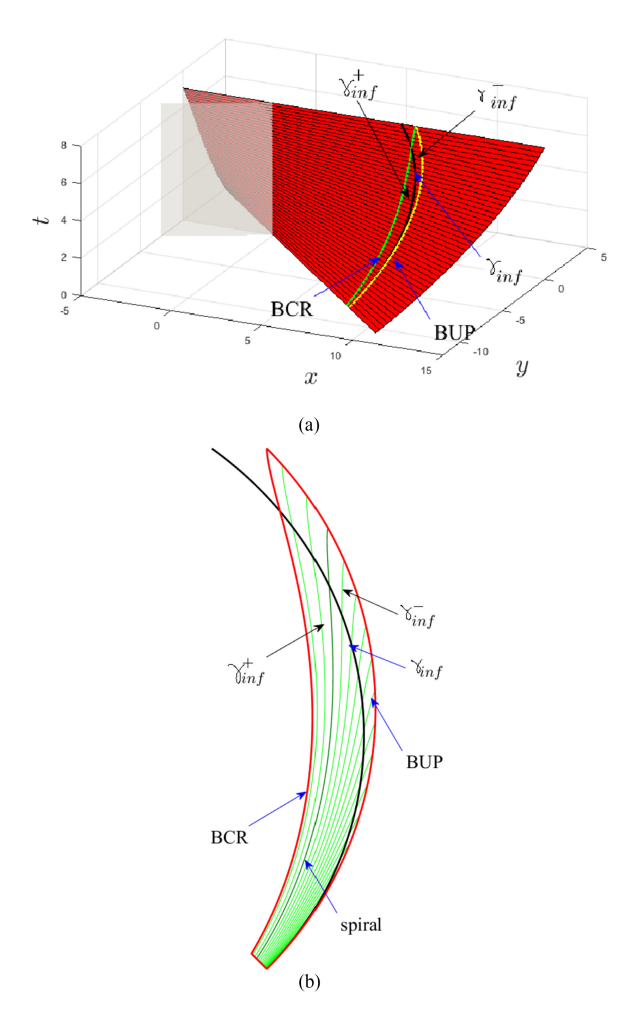


Fig. 8. (a) Locus of the inflection points in the transition region in the x-y-t space, and the partition of the transition region on $S_{\rm bar}$. (b) Projection of the inflection points and the partitions of the transition region in the x-y plane.

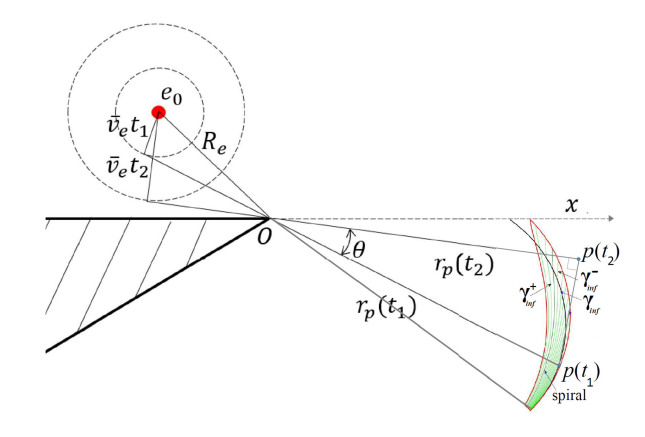


Fig. 9. Evolution of the reachability set of the evader as the pursuer moves on a straight line path reaching termination.

the beginning of the ST path. Let the ST path terminate orthogonally with the bar at time t_2 . Fig. 9 illustrates the evader's reachable disk and pursuer's trajectory between t_1 and t_2 . Note that the pursuer is on the bar at t_1 as well as t_2 .

9

From Fig. 9, we can conclude that $r_p(t_1)\sin\theta=\bar{v}_p(t_2-t_1)$ where $\theta=\cos^{-1}\frac{\bar{v}_e\,t_1}{R_e}-\cos^{-1}\frac{\bar{v}_e\,t_2}{R_e}$. Since $\sin(A-B)=\sin A\cos B-\cos A\sin B$, we obtain the following equation:

$$\frac{\bar{v}_p(t_2 - t_1)}{r_p(t_1)} = \frac{\sqrt{R_e^2 - \bar{v}_e^2 t_1^2}}{R_e} \cdot \frac{\bar{v}_e t_2}{R_e} - \frac{\bar{v}_e t_1}{R_e} \cdot \frac{\sqrt{R_e^2 - \bar{v}_e^2 t_2^2}}{R_e}.$$
(15)

Squaring both sides of (15) leads to the following quadratic equation in t_2/t_1 after simplification:

$$A\left(\frac{t_2}{t_1}\right)^2 + B\left(\frac{t_2}{t_1}\right) + C = 0 \tag{16}$$

where $A=\alpha^2+\beta^2-2\alpha\beta\cos\gamma$, $B=-2\beta(\beta-\alpha\cos\gamma)$, $C=\beta^2-\alpha^2$ and $\alpha=\frac{r_p(t_1)}{R_e}$, $\beta=\frac{\bar{v}_p}{\bar{v}_e}$, $\sin\gamma=\frac{\bar{v}_e\,t_1}{R_e}$. We obtain that $B^2-4AC=4\alpha^2(\alpha-\beta\cos\gamma)^2$, therefore, the roots of (16) are as follows:

$$\frac{t_2}{t_1} = \frac{-B \pm \sqrt{B^2 - 4AC}}{2A} = \frac{\beta^2 - \alpha^2}{\alpha^2 + \beta^2 - 2\alpha\beta\cos\gamma} \text{ or } 1.$$
(17)

This suggests that the first root provides the relation between t_1 and t_2 . So we have

$$t_2 = t_1 \frac{\beta^2 - \alpha^2}{\alpha^2 + \beta^2 - 2\alpha\beta\cos\gamma}.$$
 (18)

Since $\frac{\bar{v}_p}{r_p(t_1)} > \frac{\bar{v}_e}{r_e(t_1)} > \frac{\bar{v}_e}{R_e}$, we conclude that $\beta > \alpha$. Therefore, t_2 in (18) is positive.

Next, we show that if the pursuer follows an ST path to termination from an initial point $p(t_1) \in \gamma_{\inf}^+ \cup \gamma_{\inf}$ then $\dot{\omega}_p(t) < 0$, and $\dot{\omega}_e(t) > 0$ in $[t_1, t_2]$, which implies that the pursuer can maintain visibility of the reachable set of the evader from t_1 to t_2 .

Since $\dot{\omega}(t)=\omega^3 t$ and $\omega>0$, $\dot{\omega}(t)>0$. From Fig. 9, we can infer that $\omega_p(t)=\frac{\bar{v}_p\,r_p\,(t_2)}{r_p^2(t)}=\frac{\bar{v}_p\,r_p\,(t_2)}{r_p^2(t_2)+\bar{v}_p^2\,(t_2-t)^2}$ where t_2 and $r_p(t_2)$ are functions of t_1 , and are independent of t. Differentiating with respect to time leads to the following:

$$\dot{\omega}_p(t) = -\frac{2r_p(t_2)\bar{v}_p^3[r_p^2(t_2) - 3(t_2 - t)^2\bar{v}_p^2]}{[r_p^2(t_2) + (t_2 - t)^2\bar{v}_p^2]^3}.$$
 (19)

In order to prove $\dot{\omega}_p(t) < 0$, we need to show that $r_p^2(t_2) - 3(t_2 - t)^2 \bar{v}_p^2 > 0$. Substituting

$$r_p(t_2) = \sqrt{r_p^2(t_1) - \bar{v}_p^2(t_2 - t_1)^2},$$

the previous statement is equivalent to $r_p^2(t_1) - \bar{v}_p^2(t_2 - t_1)^2 - 3(t_2 - t)^2 \bar{v}_p^2 > 0 \Rightarrow \omega_p'(t) < 0$. Since $t > t_1$, it is sufficient to prove the following inequality:

$$r_p^2(t_1) - 4\bar{v}_p^2(t_2 - t_1)^2 > 0 \Rightarrow \frac{r_p(t_1)}{2\bar{v}_p t_1} > \frac{t_2}{t_1} - 1.$$
 (20)

Substituting the expression for t_2 from (18) into the right inequality above leads to the following quadratic inequality after

simplification:

$$r_p^2(t_1) + 2\bar{v}_p \left(2t_1 - \frac{1}{\omega(t_1)}\right) r_p(t_1) + \bar{v}_p^2 \left(\frac{R_e^2}{\bar{v}_e^2} - \frac{4t_1}{\omega(t_1)}\right) > 0.$$
(21)

We need to show that the above-mentioned inequality is satisfied for $r_p \geq r_{\rm inf}$. Since the left hand side of (21) is a convex function of r_p , the aforementioned statement is true if $r_{\rm inf}$ is greater than the larger of the two roots of the quadratic equation $((-2\pm\sqrt{3})\bar{v}_pt_1+\frac{\bar{v}_p}{\omega_e(t_1)})$ obtained by substituting the inequality in (21) with an equality. Therefore, we need to show that

$$(-2 + \sqrt{3})\bar{v}_p t_{s1} + \frac{\bar{v}_p}{\omega(t_1)} < r_{\inf}.$$
 (22)

From (28), (22) reduces to the following inequality:

$$-2 + \sqrt{3} < \frac{2}{\omega t_1 \sqrt{\omega^2 t_1^2 + 4}} - \frac{1}{\omega t_1}.$$
 (23)

To show that the inequality in (23) holds, we compute the minimum value that the R.H.S can attain. Let $s=\omega t_1\in(0,\infty)$. We need to find the minimum of $F(s)=\frac{2}{s\sqrt{s^2+4}}-\frac{1}{s}$. Taking derivative of F(s) and setting it to zero, we obtain

$$\frac{dF}{ds} = \frac{(s^2+4)^{3/2} - 4s^2 - 8}{s^2(s^2+4)^{3/2}} = 0 \Rightarrow s = \sqrt{2\sqrt{5} + 2}. \quad (24)$$

Since $\frac{dF}{ds} < 0$ for $0 < s < \sqrt{2\sqrt{5} + 2}$, and $\frac{dF}{ds} > 0$ for $s > \sqrt{2\sqrt{5} + 2}$, we obtain the $\min F(s) \approx -0.15 > -2 + \sqrt{3}$ at $s = \sqrt{2\sqrt{5} + 2}$. Therefore, inequality (23) holds for all points after the inflection point. This proves the lemma.

Corollary 1: If the pursuer cannot reach S^* (the star region), the last segment in the optimal trajectory cannot be C.

Proof: If the game terminates on a C curve, the pursuer has to be on the BUP at termination. From Property 1, there exists an interval of time just before termination for which the pursuer lies in γ_{\inf}^+ . Lemma 3 states that the pursuer should follow an ST to terminate the game from such a point.

Proof of Proposition 2: From Lemma 3, we can conclude that the optimal path from any point on $\gamma_{\inf} \cup \gamma_{\inf}^-$ is ST. Moreover, from Lemma 2, we can conclude that if the optimal trajectory starting from any point on the x-y plane reaches the transition region on an ST path, it must switch to a spiral in the transition region else the optimal path will contain an ST*ST path, which is not allowable according to Lemma 1. Additionally, from Lemma 3 and Property 5, we can conclude that from a point in the γ_{\inf}^+ , a C curve to γ_{\inf} followed by an ST curve is a candidate optimal trajectory. Therefore, we can conclude that the optimal path from any point in the transition region belongs to the family $\{C-ST,ST\}$. Moreover, from Property 4 and Property 5, the point at which it transitions from C to ST should lie in $\gamma_{\inf}^- \cup \gamma_{\inf}$ for a C-ST path to be optimal.

From Proposition 2, we obtain a partition of transition region (based on the pursuer's strategy) in Fig. 10(b). The green curve separates Region 1 into two parts. In the lower part, the optimal strategy for the pursuer is to stay on the spiral until the green curve. In the upper part, the pursuer should move on a straight line orthogonal to the terminal line (toward point M).

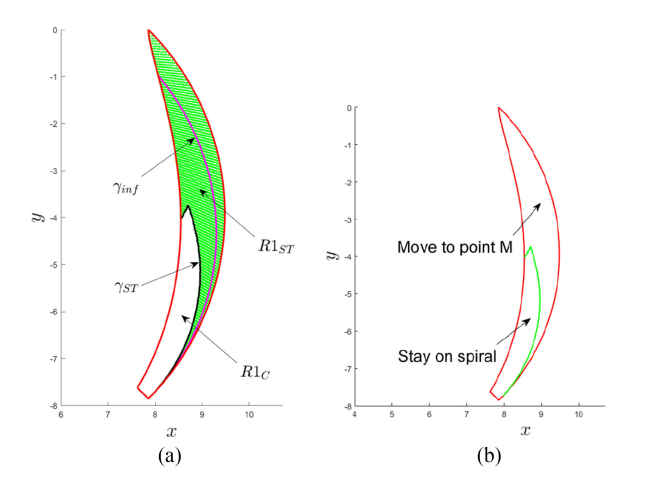


Fig. 10. Partition of the transition region based on optimal strategy of the pursuer. Initially, the optimal strategy of the pursuer is to stay on the spiral (C). Once it crosses a critical curve γ_{ST} , its optimal strategy is to move on a straight line (ST) to termination.

VI. STRATEGY FROM THE BEGINNING OF THE GAME

In this section, we present an algorithm to generate optimal paths for the pursuer from t=0, i.e., when the pursuer lies on the x-y plane. As mentioned in Section IV, the complete solution to the problem involves solving the reachability problem to the star region and the optimal trajectory to termination. First, we solve the reachability problem by computing the backward reachable sets [64] from the x-t plane to the x-y plane. To compute the backward reachable sets, the algorithm first checks if the x-axis is reachable by the pursuer. This can be done by computing the intersection of the x-axis and the circle centered at the pursuer's initial position with radius \bar{v}_nT . If they do not intersect, the pursuer cannot reach the star region. If the intersection exists, then all points on the x-axis that lie in the circle are candidate terminal positions of the pursuer. The algorithm finds a path to S^* by searching for a feasible STpath from the initial position of the pursuer to these terminal positions.

Next, we compute the optimal trajectory for the remaining points on the x-y plane by investigating the intersection of S_p and $S_{\rm bar}$. Finding the optimal trajectory to termination is based on computing the intersection between the reachable set of the pursuer in the x-y plane, and the terminal manifold. Depending on the partition of the terminal manifold in which the intersection points lie, we determine the strategy of the pursuer from the beginning of the game until termination. Based on the results of the analysis in the previous section, we can conclude that the candidate optimal trajectories for the pursuer are $\{ST, C-ST, ST-C-ST\}$. The following steps summarize the order in which the candidates are checked in order to compute the optimal trajectory.

- 1) If a feasible orthogonal straight line exists then it is the optimal strategy, where orthogonality refers to the property obtained in Proposition 1.
- 2) If the reachable cone of the pursuer intersects with the capture region, then the pursuer can follow the path ST-C to reach the star region.

```
Algorithm 1: Pursuer's Strategy for Evader in the Second Quadrant.
```

1: Note: all strategies considered must maintain visibility

```
by default.
 2: Let T = |y_e(0)|/\bar{v}_e and obtain Region 2.
 3: if y_p(0 >= 0) then
       Strategy leftarrow Shortest ST to S^*.
 5:
       return Strategy.
 6: end if
 7: if p_0 lies in Region 2 then
       Strategy \leftarrow C.
 9:
       return Strategy
10: end if
11: if there exists a ST to S^* then
        Strategy \leftarrow ST to S^*
13: else if there exists a ST orthogonal to some l_t, with
     t < T then
       Strategy \leftarrow ST \perp l_t for less than T
14:
15: else
       if there exists a ST - C - ST to S^* then
16:
          Strategy \leftarrow ST - C - ST to S^*.
17:
18:
19:
          Strategy \leftarrow ST - C - ST for less than T.
20:
       end if
21: end if
22: return Strategy
```

3) If conditions in 1) and 2) are not satisfied, the optimal path is ST-C-ST. The ST path that reaches the innermost spiral in the transition region is the initial segment of the optimal path. After the pursuer reaches the transition region, it follows the spiral, and subsequently, transitions to an ST path at the first instant at which it becomes feasible.

Algorithm 1 presents the complete procedure of finding a partition of the x-y plane based on the trajectory followed by the pursuer. Fig. 11(b) shows the partition of the x-y plane based on the trajectory followed by the pursuer, and the instantaneous vector field generated by the corresponding strategy with a=0.6. The evader's initial position is represented by the red dot. The black curves represent the boundary of Region 1. Fig. 11(a) shows the partition of the x-y plane based on the outcome. The pursuer wins the game from an initial position if it succeeds in reaching the star region while ensuring $R(t) \in V(p(t))$. If the pursuer cannot ensure the aforementioned outcome from an initial position, then it belongs to the winning region of the evader.

A. Evader-Based Partitions in Other Quadrants

In the previous section, we analyzed the tracking problem for an initial position of the evader in the second quadrant. In this section, we present the evader-based partition for the remaining initial positions of the evader. For an initial evader position in the second quadrant, the game can terminate in two ways. (i) The evader can break the LOS with the pursuer around the corner.

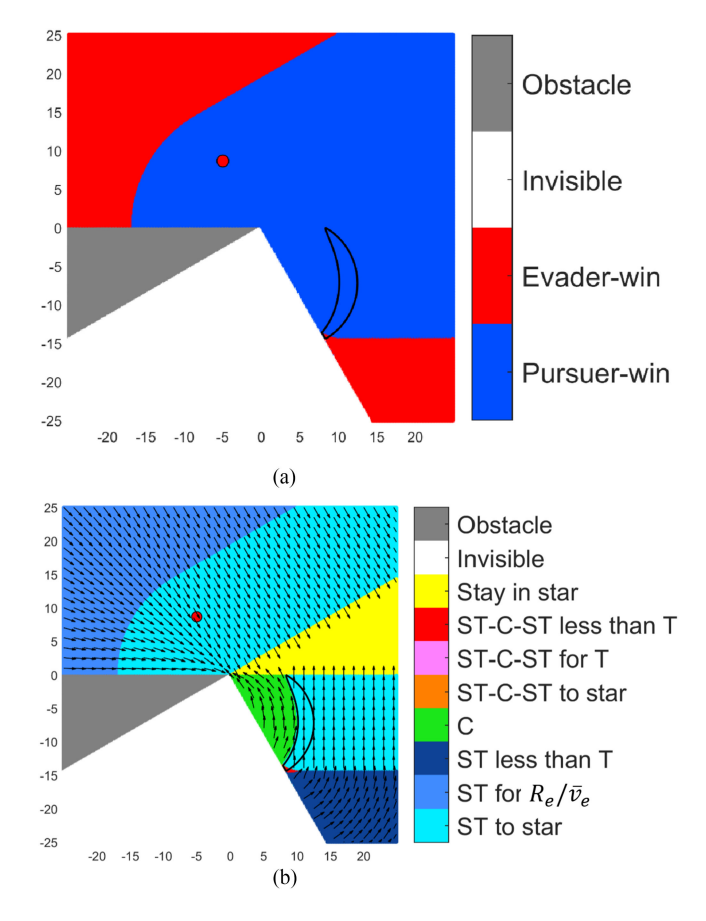


Fig. 11. Partition of the workspace around a corner based on the winner of the game and the optimal strategy of the pursuer when the evader initially lies in the second quadrant $(\phi_e(0) = \frac{2\pi}{3})$. The black curve denotes the boundary of the transition region. (a) Winner-based partition. (b) Strategy-based partition and vector field.

(ii) The evader can reach the corner before the pursuer reaches the star region, and immediately break LOS by moving along the edge not visible to the pursuer. Fig. 12(b) shows an initial evader position (e) in the first quadrant. Let T denote the time it takes for R(t) to touch the corner. An important difference in this scenario from the one in which the evader is in the second quadrant is that the terminal position of the bar l_T is not aligned with the star region. Therefore, the pursuer might be able to maintain visibility of R(t) until time T without reaching the star region in which case the evader will follow the strategy (ii) to terminate the game. The region enclosed between l_T and the x-axis is the set of such terminal positions of the pursuer. Lines 26–32 perform the aforementioned check in Algorithm 2 that summarizes the procedure for any evader position in the first quadrant.

Fig. 13(a) shows the partition of the plane based on the winner for an initial position of the evader in the first quadrant. Fig. 13(b) shows the partition of the plane based on the strategy of the pursuer. Fig. 14(a) and (b) present the winning partition and the strategy of the pursuer for an initial position of the evader in the star region.

We observe that in Fig. 11(b), region for ST - C - ST for T does not exist, whereas in Figs. 13(b) and 14(b), there is

```
Algorithm 2: Pursuer's Strategy for Evader in the First Quadrant.
```

```
1: Note: all strategies considered must maintain visibility
     by default.
 2: Let T = R_e/\bar{v}_e and obtain Region 2.
 3: if p_0 lies in the same half-space as e_0 separated by l_T
       Strategy \leftarrow Shortest ST to S^*.
 4:
 5:
       return Strategy.
 6: end if
 7: if p_0 lies in Region 2 then
 8:
       Strategy \leftarrow C.
 9:
       return Strategy
10: end if
11: if there exists a ST to l_T then
       Strategy \leftarrow ST to l_T
12:
13: else if there exists a ST orthogonal to some l_t, with
     t < T then
       Strategy \leftarrow ST \perp l_t for less than T
14:
15:
       return Strategy
16: else
       if there exists a ST - C - ST to S^* then
17:
18:
          Strategy \leftarrow ST - C - ST to S^*.
19:
       else if there exists a ST - C - ST to l_T then
          Strategy \leftarrow ST - C - ST for time T.
20:
21:
22:
          Strategy \leftarrow ST - C - ST for less than T.
23:
       end if
24:
       return Strategy
25: end if
26: if Strategy = ST to l_T then
27:
       if there exists a ST to S^* then
28:
          Strategy \leftarrow ST to S^*.
29:
       else if there exists a ST - C - ST to S^* then
          Strategy \leftarrow ST - C - ST to S^*.
30:
31:
       end if
32: end if
33: return Strategy
```

a tiny region of ST-C-ST for T between the other two ST - C - ST regions. There are two Region 1 in Figs. 13(b) and 14(b), since the evader can escape by either moving in the clockwise direction or counter-clockwise direction based on the pursuer's position. In C (green) regions, the pursuer has more than one strategy to reach the star region and track the evader forever. So "optimal strategy" cannot be defined in terms of tracking time. Therefore, we only present a feasible strategy for the region. The green region is the projection of the pursuer-win region of the red surface on the xy-plane. If the pursuer initially lies in this region, it can follow a simple strategy: wait for the bar to reach it and get on the red surface, then it follows the strategy we obtained for the pursuer-win region of the surface. In other words, if the pursuer lies in Region 2, it can follow the spiral to the star region (C). Similarly, in all pursue-win regions, strategies we provide are feasible ones for the pursuer to reach S^* (the star region).

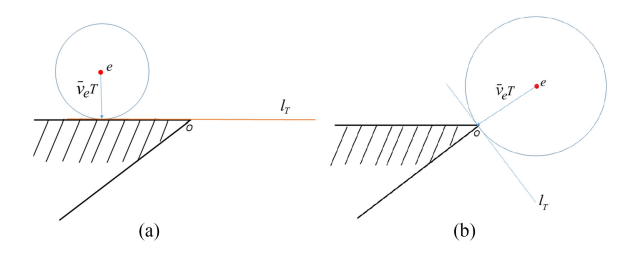


Fig. 12. Reachability set for two different initial positions of the evader. (a) If the evader is initially located in the third quadrant, the reachability set first touches the edge of the obstacle as time progresses. (b) If the evader is initially located in the second quadrant, the reachability set first touches the corner of the obstacle as time progresses.

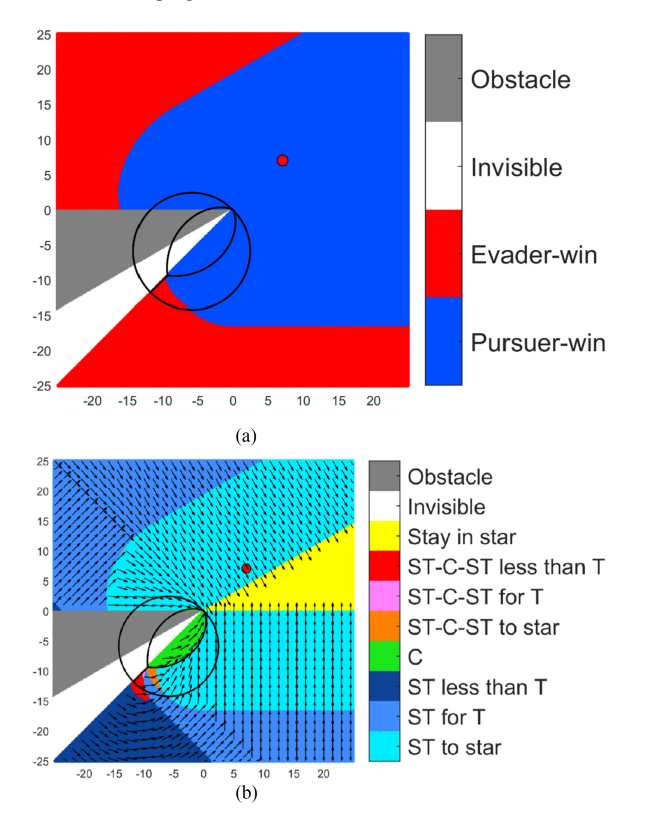


Fig. 13. Partition of the workspace around a corner based on the winner of the game and the optimal strategy of the pursuer when the evader initially lies in the first quadrant ($\phi_e(0) = \frac{\pi}{2}$). The black curve denotes the boundary of the transition region. (a) Winner-based partition. (b) Strategy-based partition and vector field.

B. Discussion

In the previous section, we have addressed a target-tracking problem around a corner. In this section, we compare the results in this paper with previously known solutions to variations of the problem formulation under consideration in this paper.

The optimal control policy of the players in a game depends on the information available to the players. Fig. 15 shows the evader-based partition for an observer with knowledge about the current velocity of the target [11]. In this paper, we assume that the observer has knowledge about the current position of the target. This changes the nature of the optimal solutions and the partitions as is evident from Figs. 11(b) and 15. For example, the observer's control policy in Region 4 explicitly

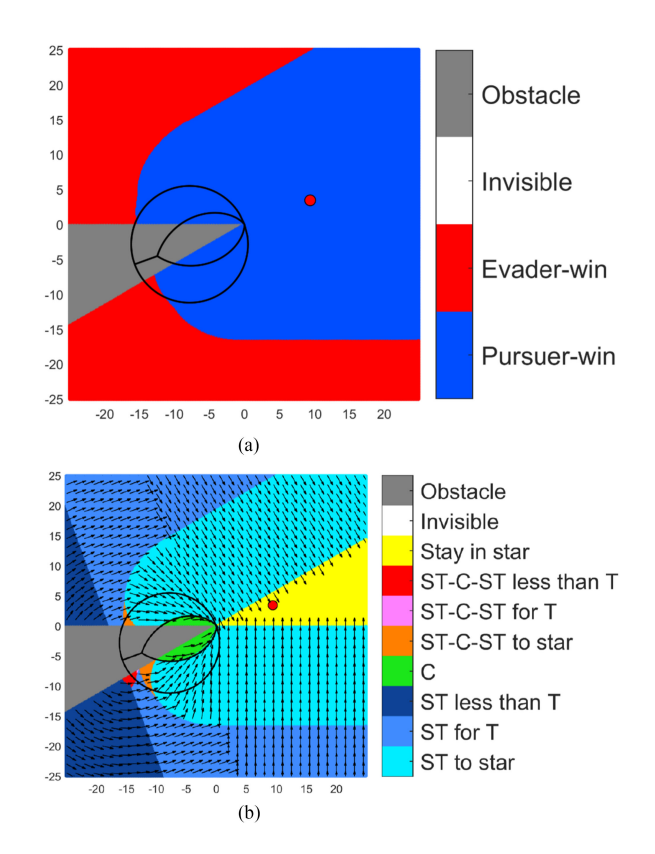


Fig. 14. Partition of the workspace around a corner based on the winner of the game and the optimal strategy of the pursuer when the evader initially lies in the star region (S^*) . The black curve denotes the boundary of the transition region. (a) Winner-based partition. (b) Strategy-based partition and vector field.

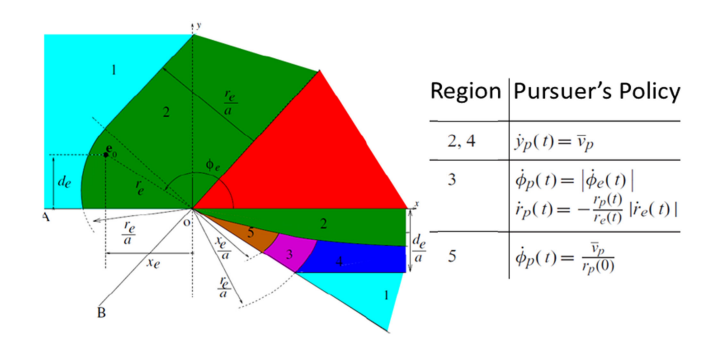


Fig. 15. Evader-based partition around the corner and the corresponding strategies of the pursuer around the corner.

depends on the current velocity of the target in Fig. 15. It is easier to estimate the current position of a non-cooperative target than to estimate its instantaneous velocity. Therefore, the problem formulation considered in this paper is a step closer to reality. In spite of the differences in the observer's optimal strategy, the evader-win regions in both partitions (Region shaded red in 11(a) and Region 1 in Fig. 15) bear some similarities. We can show that the evader-win region in Fig. 15 is a subset of the evader-win region in Fig. 11(a). Therefore, the algorithm presented in [11] for computing the bounded polygonal region that contains the pursuer-win region in an environment containing multiple obstacles (called the U-set) also works for the problem formulation in this paper.

VII. CONCLUSION

In this paper, we addressed the path planning problem for a mobile observer that tries to maintain an LOS with a mobile target in an environment containing multiple obstacles. The concept of dominant strategy reduces the game into an optimal control problem. The mixed constraints posed by the obstacles is solved by lifting the problem in space-time coordinates. We showed that the optimal trajectories for the observer belongs to the family $\{ST, C - ST, ST - C - ST\}$. We presented a partition of the workspace around the corner based on the optimal trajectory of the observer.

Next, we provide some future directions of research.

- 1) Higher order motion models: The framework presented in this paper is general, and can be applied to observers with higher order motion models and non-holonomic constraints. In [65], we have presented necessary conditions for persistent tracking for an observer modeled as a Dubins car, Reed–Shepp, and DDR. In the future, we will build a potential-field-based planner from the vector fields presented in this paper.
- 2) Multirobot motion planning: Multiple points of view add extra information on the target resulting in a better estimate of its position. The vector fields can be used to guide a team of observers to track a team of targets. Since the vector fields are generated by a single target, an allocation problem arises among the observers in case of multiple targets. Although, centralized [66] as well as decentralized [67] approaches have been proposed for multirobot allocation problems, their performance in dynamic scenarios is an important problem that needs to be addressed in the future.
- 3) Discrete abstractions: An interesting direction of future research is to design sequential [68] and hybrid controllers [69] for the problem of target tracking. Previous efforts have primarily focused on the problem of designing such planners for a robot to reach a goal. There have been some efforts in the past to design controllers for the search problem [70]. In [71], we presented hybrid controllers for multiple observers tracking a single target using event-triggered strategies. In the future, we plan to design such controllers for single/multiple observers using the concept of pursuit fields.

Additionally, incorporating sensing constraints, for example, limited FOV and limited range, would be some interesting future directions. Finally, designing a potential-field-based planner that can also account for the dimensions of the observer robot is another future research direction.

APPENDIX

A. Proof of Property 1, Property 4, and Property 5

Proof of Property 1: In Fig. 8(b), the green curves represent some spirals originating from t=0 plane in Region 1. $\gamma_{\rm inf}$ (black curve) represents the locus of the inflection points of each spiral. We will obtain the mathematical expression of $\gamma_{\rm inf}$ as a function of t.

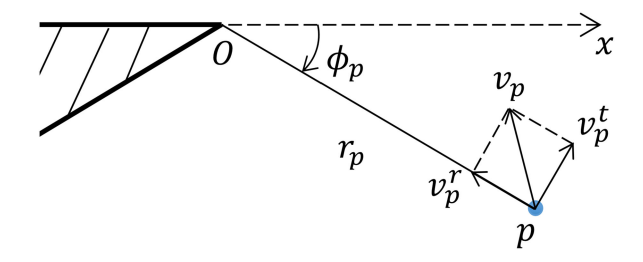


Fig. 16. Tangential and radial velocity of the pursuer in the polar coordinates attached to the corner.

Refer to Fig. 16. The heading angle of the pursuer h(t) is given by the following expression:

$$h(t) = \tan^{-1}\left(\frac{v_p^r}{v_p^t}\right) + \frac{\pi}{2} + \phi_p.$$
 (25)

Substituting $v_p^r=\sqrt{\overline{v}_p^2-{v_p^t}^2}$ and $v_p^t=\omega_p r_p$ in (25), where ω_p is the angular velocity of the pursuer about the origin, leads to the following equation:

$$h(t) = \tan^{-1}\left(\sqrt{\frac{\bar{v}_p^2}{\omega_p^2 r_p^2} - 1}\right) + \frac{\pi}{2} + \phi_p$$
 (26)

Using the facts that $\dot{\phi}_p = \omega(t)$ on the spiral, and $\omega'(t) = \frac{\bar{v}_s^3 t}{(R_c^2 - \bar{v}_c^2 t^2)^{3/2}} = \omega^3 t$, we obtain the following expression for the derivative of h(t) with respect to time:

$$\dot{h}(t) = \omega \left(\frac{\omega^2 r_p t}{\dot{r}_p} + 2 \right). \tag{27}$$

From (27), we can see that $\dot{h}(0)>0$, which implies that the curvature of the spiral is positive in the beginning. Since $v_p^r(t)\to 0$ near termination, $\dot{h}(t)$ is negative before termination, which implies that the spiral has a negative curvature before termination. From the definition of inflection point $(\dot{h}(t)=0)$, we obtain the following expression for r_p :

$$r_p = \frac{2\bar{v}_p}{\omega\sqrt{\omega^2 t^2 + 4}}.$$
 (28)

Proof of Property 4: Consider two initial positions for the pursuer, $p_1(t_1)$ and $p_2(t_1)$ on the same bar such that $r_{p_1}(t_1) < r_{p_2}(t_1)$. Let $\gamma_1(t)$ and $\gamma_2(t)$ be the trajectory for the pursuer when it follows the differential equations $\dot{\phi}_p(t) = \omega(t), \quad \dot{r}_p(t) = -\sqrt{\bar{v}_p^2(t) - r_p^2(t)\omega^2(t)}$ with initial condition $p_1(t_1)$ and $p_2(t_1)$, respectively. The differential equations govern the evolution of the pursuer's trajectories from the two initial conditions when it maintains the same angular speed $(\omega(t))$ and total speed $(\bar{v}_p(t))$ on both of them. From Cauchy-Lipschtiz theorem [63], the differential equation has a unique solution for each initial condition. Therefore, $r_{p_1}(t) < r_{p_2}(t)$ for all $t \geq t_1$. Let t_2 denote the time at which $\gamma_2(t)$ terminates $\Rightarrow r_{p_2}(t_2)\dot{\phi}_p(t_2) = \bar{v}_p$. Since $r_{p_1}(t_2) < r_{p_2}(t_2)$, the tangential velocity $r_{p_1}(t_2)\dot{\phi}_p(t_2) < r_{p_2}(t_2)\dot{\phi}_p(t_2) = \bar{v}_p$. Therefore, if the pursuer follows γ_1 , it can avoid termination at t_2 since the

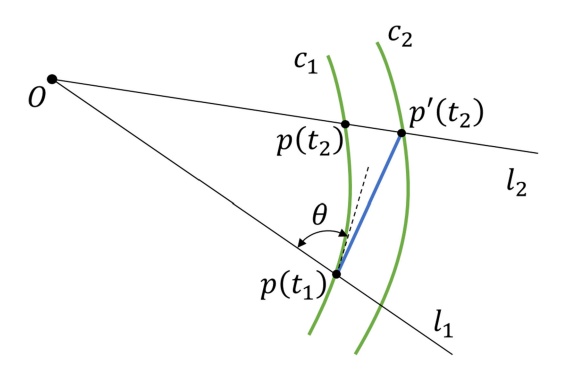


Fig. 17. Possible trajectories of a pursuer initially located at $p(t_1)$ which lies on a spiral c_1 . For any path other than C, the pursuer would eventually land up on an outer spiral.

tangential component of its velocity is less than \bar{v}_p , and hence, track for a longer time.

Proof of Property 5: Refer to Fig. 17. O is the origin/corner. Initially, the pursuer is located at $p(t_1)$ that lies on spiral c_1 . When the pursuer moves on the spiral, it matches its tangential velocity with the rotating bar l_1 , and moves radially inward with the maximum possible speed (toward the origin while maintaining a maximum speed of \bar{v}_p). Any other trajectory for the pursuer on the spiral that can maintain visibility has a smaller radial velocity toward the origin. Therefore, for any other trajectory, the angle between the pursuer's heading and the bar at t_1 must be greater than θ , which is the angle between its heading on the spiral and the bar. If the pursuer moves on a straight line path (blue line in the figure) from t_1 , then spiral c_1 "swings" to the left of the straight line path due to its positive curvature in γ_{inf}^+ . Therefore, when they arrive on the same bar at t_2 , the straight line path will end on spiral c_2 at $p'(t_2)$, which is farther from the origin than $p(t_2)$ on c_1 .

B. Inactive Boundary Constraints¹

Here, we analyze the problem when the boundary constraint is inactive (i.e., $\mu=0$). The corresponding Hamiltonian function is as follows:

$$H = -1 + p_1 \frac{\bar{v}_e}{\sqrt{R_e^2 - (\bar{v}_e t)^2}} + u_2 \left(-p_2 \sin u_1 + \frac{p_3}{x_2} \cos u_1 \right)$$
(29)

$$= -1 + p_1 \frac{\bar{v}_e}{\sqrt{R_e^2 - (\bar{v}_e t)^2}} + \left\{ \sqrt{\frac{p_3^2}{x_2^2} + p_2^2} \right\} u_2 \cos(u_1 + \alpha)$$
(30)

where $\sin \alpha = \frac{p_2}{\sqrt{\frac{p_3^2}{x_2^2} + p_2^2}}$. Since $u_1 \in [0, 2\pi)$, $\cos(u_1 + \alpha)$ can

take any value in the range [-1,1]. Therefore, u_2^* is given by

$$u_2^* = \begin{cases} 0 & \text{if } \cos(u_1 + \alpha) > 0\\ \text{any value in [0,1]} & \text{if } \cos(u_1 + \alpha) = 0\\ \bar{v}_p & \text{if } \cos(u_1 + \alpha) < 0 \end{cases}$$
(31)

From (31), we can conclude that the optimal value of u_2 that minimizes the Hamiltonian (and the product $u_2 \cos(u_1 + \alpha)$) is $u_2^* = \bar{v}_p$. Moreover, u_1 that minimizes the Hamiltonian is given by the following expression:

$$\frac{\partial H}{\partial u_1}\Big|_{u_1=u_1^*(t)} = -p_2^* \bar{v}_p \cos u_1^* - p_3^* \frac{\bar{v}_p}{x_2^*} \sin u_1^* = 0$$

$$\Rightarrow \tan u_1^* = -\frac{p_2^*}{p_2^*} x_2^*. \tag{32}$$

Next, we show that the optimal trajectory of the pursuer in free space is a straight line. Let (x_p, y_p) denote the position of the pursuer in Cartesian coordinates. The equations of motion for the pursuer in Cartesian coordinates is given as follows:

$$\dot{x}_p = -\bar{v}_p \sin(u_1 + x_3), \qquad \dot{y}_p = \bar{v}_p \cos(u_1 + x_3).$$
 (33)

Differentiating both sides of (32) with respect to time leads to the following:

$$\dot{u}_1^* = \bar{v}_p \frac{p_2^*}{p_2^*} \sin u_1^* \cos^2 u_1^* - \frac{\bar{v}_p}{x_2^*} \cos^3 u_1^*. \tag{34}$$

Therefore, we obtain the following:

$$\dot{u}_1^* + \dot{x}_3^* = \frac{1}{2}\bar{v}_p \sin(2u_1^*) \left(\frac{p_2^*}{p_3^*} \cos u_1^* + \frac{1}{x_2^*} \sin u_1^*\right) = 0.$$

The right-hand side equality comes from (32). Therefore, $u_1^* + x_3^*$ is a constant and $(x_p^*(t), y_p^*(t))$ lies on a straight line passing through the point $(R_p \cos \phi_p(0), R_p \sin \phi_p(0))$ with slope $-\cot(u_1^* + x_3^*)$. Therefore, the pursuer's optimal strategy when the boundary constraint is inactive is always a line segment.

When boundary constraints are inactive, the Hamiltonian is defined as in (30). The costate equation is thus given by the following:

$$\dot{\mathbf{p}}^{*}(t) = -\left. \frac{\partial H}{\partial \mathbf{x}} \right|_{(\mathbf{x}^{*}, \mathbf{u}^{*})}$$

$$\Rightarrow \dot{p}_{1}^{*} = 0, \quad \dot{p}_{2}^{*} = p_{3} \frac{u_{2}^{*}}{x_{2}^{*}} \cos u_{1}^{*}, \quad \dot{p}_{3}^{*} = 0. \quad (35)$$

When boundary constraints are inactive, the pursuer's trajectory is a straight line. Consider the case when the game ends with the pursuer moving on "ST." From the equality terminal condition in (6), we can obtain the following transversality condition:

$$\mathbf{p}^*(t_f^*) = \alpha_1 \frac{\partial g}{\partial \mathbf{x}}(\mathbf{x}^*(t_f^*), t_f^*)$$
(36)

where $\alpha_1 \neq 0$. Therefore, we obtain the following:

$$p_1^*(t_f) = \alpha_1, \ p_2^*(t_f) = 0, \ p_3^*(t_f) = -\alpha_1$$

 $\Rightarrow p_1^*(t) = \alpha_1, \ p_3^*(t) = -\alpha_1.$

the following expression:

¹The analysis in Appendix B has appeared in part in [62].

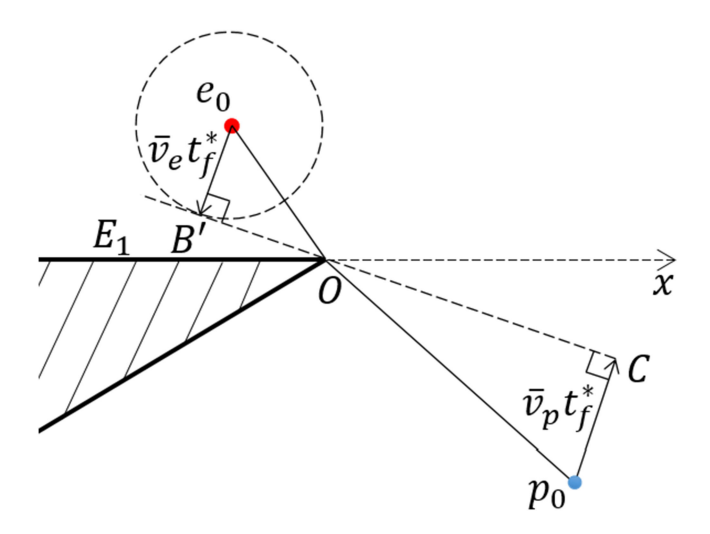


Fig. 18. Termination on ST.

Substituting $p_2^*(t_f^*) = 0$ into (32), we obtain $u_1^*(t_f^*) = 0$. So the pursuer's velocity only has a tangential component (v_p^t) at termination. Moreover, since the pursuer is on the bar at termination, $v_p(t_f^*)$ is orthogonal to the terminal bar. Since we did not include the inequality terminal condition (7) in the transversality condition, we will now check that it is satisfied whenever (6) is satisfied at termination. Fig. 18 illustrates the pursuer's trajectory and the evader's reachable disk when the game ends with inactive boundary constraints.

From $\triangle Oe_0B'$ and $\triangle Op_0C$ in Fig. 18, we obtain the following relations:

$$\frac{\bar{v}_e t_f}{\sqrt{R_e^2 - (\bar{v}_e t_f)^2}} = \tan(\tilde{\phi}_e(t_f) - \tilde{\phi}_e(0))$$
$$\frac{\bar{v}_p t_f^*}{x_2^*(t_f^*)} = \tan(\phi_p(t_f^*) - \phi_p(0)).$$

Since $\phi_e(t_f^*) - \phi_p(t_f^*) = \pi$ and $\phi_e(0) - \phi_p(0) < \pi$, we obtain $\phi_e(t_f^*) - \phi_e(0) > \phi_p(t_f^*) - \phi_p(0)$. Therefore

$$\frac{\bar{v}_e}{\sqrt{R_e^2 - (\bar{v}_e t_f^*)^2}} > \frac{\bar{v}_p}{x_2^*} \tag{37}$$

which is the same as (7) given that $u_2^* = \bar{v}_p$ and $u_1^*(t_f^*) = 0$. Therefore, we have proved that (7) is automatically satisfied when (6) is satisfied.

Next, we want to solve for t_f^* when boundary constraints are inactive. We obtain the following equation from the geometry in Fig. 18:

$$\sin^{-1}\frac{\bar{v}_e t_f^*}{R_e} - \sin^{-1}\frac{\bar{v}_p t_f^*}{R_p} = \pi - \phi_e(0) + \phi_p(0) = \Delta\phi_0 \quad (38)$$

where $\Delta \phi_0$ is a constant value. Solving for (38) leads to a unique positive solution for t_f^* as follows:

$$t_f^* = \frac{R_e R_p \sin(\Delta \phi_0)}{\sqrt{R_p^2 \bar{v}_e^2 + R_e^2 \bar{v}_p^2 - 2R_e R_p \bar{v}_e \bar{v}_p \cos(\Delta \phi_0)}}.$$
 (39)

Therefore, the straight line trajectory orthogonal to the terminal line is the unique optimal solution when boundary constrains are inactive.

When boundary constraints are active, the pursuer moves on the spiral. If the game ends on "C," at termination, the pursuer's velocity is also orthogonal to the terminal bar. This is true due to the fact that the pursuer cannot spare any speed in the radial direction. So, it moves in the tangential direction with maximum speed \bar{v}_p . We summarize the above discussion in the following proposition.

Proposition 3: The pursuer's velocity is always orthogonal to the bar at termination.

REFERENCES

- [1] T. Furukawa, F. Bourgault, B. Lavis, and H. F. Durrant-Whyte, "Recursive Bayesian search-and-tracking using coordinated UAVs for lost targets," in *Proc. IEEE Int. Conf. Robot. Automat.*, 2006, pp. 2521–2526.
- [2] D. Nigg, S. Alobaidi, R. Jirage, T. Deshpande, and H. Alkharboosh, "Choosing the best follow-me drone camera system for the outdoor sports enthusiast," Eng. Technol. Manage. Student Projects, Portland State Univ., Portland, OR, USA, 2017.
- [3] A. M. Khaleghi et al. "A DDDAMS-based planning and control framework for surveillance and crowd control via UAVs and UGVs," Expert Syst. Appl., vol. 40, no. 18, pp. 7168–7183, 2013.
- [4] B. Livingston, "The role of UAVs/MAVs in domestic surveillance and control," Rense. com, 2004. [Online]. Available: http://www.rense.com/general47/uav.htm
- [5] A. Rodríguez, J. J. Negro, M. Mulero, C. Rodríguez, J. Hernández-Pliego, and J. Bustamante, "The eye in the sky: Combined use of unmanned aerial systems and GPS data loggers for ecological research and conservation of small birds," *PLoS One*, vol. 7, no. 12, pp. 1–6, 2012.
- [6] K. Zhou and S. I. Roumeliotis, "Optimal motion strategies for range-only constrained multisensor target tracking," *IEEE Trans. Robot.*, vol. 24, no. 5, pp. 1168–1185, Oct. 2008.
- [7] E. W. Frew and S. M. Rock, "Trajectory generation for constant velocity target motion estimation using monocular vision," in *Proc. IEEE Int. Conf. Robot. Automat.*, 2003, vol. 3, pp. 3479–3484.
- [8] S. Bhattacharya and S. Hutchinson, "On the existence of Nash equilibrium for a two player pursuit-evasion game with visibility constraints," in *Algorithmic Foundation of Robotics VIII*. New York, NY, USA: Springer, 2009, pp. 251–265.
- [9] S. Bhattacharya and S. Hutchinson, "On the existence of Nash equilibrium for a two-player pursuit-evasion game with visibility constraints," *Int. J. Robot. Res.*, vol. 29, no. 7, pp. 831–839, Jun. 2010.
- [10] G. Owen, Game Theory. New York, NY, USA: Academic, 1995.
- [11] S. Bhattacharya and S. Hutchinson, "A cell decomposition approach to visibility-based pursuit evasion among obstacles," *Int. J. Robot. Res.*, vol. 30, no. 14, pp. 1709–1727, Sep. 2011.
- [12] S. LaValle, H. Gonzalez-Banos, C. Becker, and J.-C. Latombe, "Motion strategies for maintaining visibility of a moving target," in *Proc. IEEE Int. Conf. Robot. Automat.*, Apr. 1997, vol. 1, pp. 731–736.
- [13] D. Panagou and V. Kumar, "Cooperative visibility maintenance for leader-follower formations in obstacle environments," *IEEE Trans. Robot.*, vol. 30, no. 4, pp. 831–844, Aug. 2014.
- [14] W. Ding, M. R. Ganesh, R. N. Severinghaus, J. J. Corso, and D. Panagou, "Real-time model predictive control for keeping a quadrotor visible on the camera field-of-view of a ground robot," in *Proc. Amer. Control Conf.*, 2016, pp. 2259–2264.
- [15] S. Maniatopoulos, D. Panagou, and K. J. Kyriakopoulos, "Model predictive control for the navigation of a nonholonomic vehicle with field-of-view constraints," in *Proc. Amer. Control Conf.*, 2013, pp. 3967–3972.
- [16] K. Zhou and S. I. Roumeliotis, "Multirobot active target tracking with combinations of relative observations," *IEEE Trans. Robot.*, vol. 27, no. 4, pp. 678–695, Aug. 2011.
- [17] R. Murrieta-Cid, H. H. González-Banos, and B. Tovar, "A reactive motion planner to maintain visibility of unpredictable targets," in *Proc. IEEE Int. Conf. Robot. Automat.*, 2002, vol. 4, pp. 4242–4248.
- [18] S. Bhattacharya, S. Candido, and S. Hutchinson, "Motion strategies for surveillance," in *Proc. Robot., Sci. Syst.*, 2007, pp. 249–256.

- [19] T. Başar and G. J. Olsder, Dynamic Noncooperative Game Theory. Philadelphia, PA, USA: SIAM, 1998.
- [20] R. Isaacs, Differential Games: A Mathematical Theory With Applications to Warfare and Pursuit, Control and Optimization. New York, NY, USA: Wiley, 1965.
- [21] V. Isler and N. Karnad, "The role of information in the cop-robber game," Theor. Comput. Sci., vol. 3, no. 399, pp. 179–190, 2008.
- [22] S. Bhattacharya, T. Başar, and N. Hovakimyan, "A visibility-based pursuit-evasion game with a circular obstacle," *J. Optim. Theory Appl.*, vol. 171, no. 3, pp. 1071–1082, 2016.
- [23] S. Bhattacharya, T. Başar, and N. Hovakimyan, "Game-theoretic analysis of a visibility based pursuit-evasion game in the presence of a circular obstacle," AIP Conf. Proc., vol. 1479, no. 1., pp. 1222–1225, 2012.
- [24] S. Bhattacharya, T. Başar, and N. Hovakimyan, "Singular surfaces in multiagent connectivity maintenance games," in *Proc. Conf. Decis. Control Eur. Control Conf.*, 2011, pp. 261–266.
- [25] D. J. Balkcom and M. T. Mason, "Time optimal trajectories for bounded velocity differential drive vehicles," *Int. J. Robot. Res.*, vol. 21, no. 3, pp. 199–217, Mar. 2002.
- [26] H. Chitsaz, S. M. LaValle, D. J. Balkcom, and M. T. Mason, "Minimum wheel-rotation paths for differential-drive mobile robots," *Int. J. Robot. Res.*, vol. 28, no. 1, pp. 66–80, Jan. 2009.
- [27] P. Tokekar, N. Karnad, and V. Isler, "Energy-optimal trajectory planning for car-like robots," *Auton. Robots*, vol. 37, no. 3, pp. 279–300, Oct. 2014.
- [28] U. Ruiz, R. Murrieta-Cid, and J. L. Marroquin, "Time-optimal motion strategies for capturing an omnidirectional evader using a differential drive robot," *IEEE Trans. Robot.*, vol. 29, no. 5, pp. 1180–1196, Oct. 2013.
- [29] D. Jacobo, U. Ruiz, R. Murrieta-Cid, H. Becerra, and J. Marroquin, "A visual feedback-based time-optimal motion policy for capturing an unpredictable evader," *Int. J. Control*, vol. 88, no. 4, pp. 663–681, 2015.
- [30] R. Murrieta-Cid, U. Ruiz, J. L. Marroquin, J. P. Laumond, and S. Hutchinson, "Tracking an omnidirectional evader with a differential drive robot," *Auton. Robots*, vol. 31, no. 4, pp. 345–366, Aug. 2011.
- [31] U. Ruiz and R. Murrieta-Cid, "A differential pursuit/evasion game of capture between an omnidirectional agent and a differential drive robot, and their winning roles," *Int. J. Control*, vol. 89, no. 11, pp. 2169–2184, 2016.
- [32] P. Jacobs and J. Canny, "Planning smooth paths for mobile robots," in Nonholonomic Motion Planning. Boston, MA, USA: Springer, 1993, pp. 271–342.
- [33] J.-D. Boissonnat and S. Lazard, "A polynomial-time algorithm for computing a shortest path of bounded curvature amidst moderate obstacles," in *Proc. 12th Annu. Symp. Comput. Geom.*, 1996, pp. 242–251.
- [34] S. M. Lavalle and J. J. Kuffner, "Rapidly-exploring random trees: Progress and prospects," in *Proc. 4th Workshop Algorithmic Comput. Robot.*, New Directions, 2000, pp. 293–308.
- [35] R. Murrieta-Cid, T. Muppirala, A. Sarmiento, S. Bhattacharya, and S. Hutchinson, "Surveillance strategies for a pursuer with finite sensor range," *Int. J. Robot. Res.*, vol. 26, no. 3, pp. 233–253, 2007.
- [36] Y. Oh, S. Choi, and S. Oh, "Chance-constrained target tracking for mobile robots," in *Proc. IEEE Int. Conf. Robot. Automat.*, 2015, pp. 409–414.
- [37] L. Blackmore and M. Ono, "Convex chance constrained predictive control without sampling," in *Proc. AIAA Guid.*, *Navig. Control Conf.*, 2009, pp. 7–21.
- [38] M. R. Hestenes, Calculus of Variations and Optimal Control Theory. Hoboken, NJ, USA: Wiley, 1965.
- [39] R. V. Gamkrelidze, "On some extremal problems in the theory of differential equations with applications to the theory of optimal control," *J. Soc. Ind. Appl. Math., Ser. A, Control*, vol. 3, no. 1, pp. 106–128, 1965.
- [40] L. W. Neustadt, Optimization: A Theory of Necessary Conditions. Princeton, NJ, USA: Princeton Univ. Press, 2015.
- [41] A. Arutyunov, Optimality Conditions: Abnormal and Degenerate Problems, vol. 526. New York, NY, USA: Springer, 2013.
- [42] F. H. Clarke, Optimization and Nonsmooth Analysis. Philadelphia, PA, USA: SIAM, 1990.
- [43] F. Clarke, "The maximum principle in optimal control, then and now," Control Cybern., vol. 34, no. 3, pp. 709–722, 2005.
- [44] F. Clarke, Necessary Conditions in Dynamic Optimization, vol. 816. Providence, RI, USA: Amer. Math. Soc., 2005.
- [45] F. Clarke and M. R. De Pinho, "Optimal control problems with mixed constraints," SIAM J. Control Optim., vol. 48, no. 7, pp. 4500–4524, 2010.

- [46] N. P. Osmolovskii, Calculus of Variations and Optimal Control, vol. 180. Providence, RI, USA: Amer. Math. Soc., 1998.
- [47] Z. Páles and V. Zeidan, "Strong local optimality conditions for control problems with mixed state-control constraints," in *Proc. Conf. Decis. Con*trol, 2002, vol. 4, pp. 4738–4743.
- [48] Z. Páles and V. Zeidan, "Optimal control problems with set-valued control and state constraints," SIAM J. Optim., vol. 14, no. 2, pp. 334–358, 2003.
- [49] H. Maurer, "Numerical solution of singular control problems using multiple shooting techniques," *J. Optim. Theory Appl.*, vol. 18, no. 2, pp. 235– 257, 1976.
- [50] J. T. Betts, Practical Methods for Optimal Control and Estimation Using Nonlinear Programming. Philadelphia, PA, USA: SIAM, 2010.
- [51] H. G. Bock and K.-J. Plitt, "A multiple shooting algorithm for direct solution of optimal control problems," *IFAC Proc. Vol.*, vol. 17, no. 2, pp. 1603–1608, 1984.
- [52] J. T. Betts, "Issues in the direct transcription of optimal control problems to sparse nonlinear programs," in *Computational Optimal Control (Int. Ser. Numer. Math.)*, vol. 115. New York, NY, USA: Springer, 1994, 1994.
- [53] J. T. Betts and W. P. Huffman, "Path-constrained trajectory optimization using sparse sequential quadratic programming," *J. Guid.*, *Control*, *Dyn.*, vol. 16, no. 1, pp. 59–68, 1993.
- [54] M. De Berg, M. Van Kreveld, M. Overmars, and O. C. Schwarzkopf, "Computational geometry," in *Computational Geometry*. New York, NY, USA: Springer, 2000, pp. 1–17.
- [55] N. N. Krasovskii, "On the theory of controllability and observability of linear dynamic systems," J. Appl. Math. Mech., vol. 28, no. 1, pp. 1–14, 1964
- [56] A. B. Kurzhanski and P. Varaiya, "Dynamic optimization for reachability problems," J. Optim. Theory Appl., vol. 108, no. 2, pp. 227–251, 2001.
- [57] F. L. Chernousko, State Estimation for Dynamic Systems. Boca Raton, FL, USA: CRC Press, 1993.
- [58] J. Lygeros, C. Tomlin, and S. Sastry, "Controllers for reachability specifications for hybrid systems," *Automatica*, vol. 35, no. 3, pp. 349–370, 1999.
- [59] O. Stursberg and B. H. Krogh, "Efficient representation and computation of reachable sets for hybrid systems," in *Proc. Int. Workshop Hybrid Syst.*, *Comput. Control.*, 2003, pp. 482–497.
- [60] V. S. Patsko, S. G. Pyatko, and A. A. Fedotov, "Three-dimensional reachability set for a nonlinear control system," *J. Comput. Syst. Sci. Int.*, vol. 42, no. 3, pp. 320–328, 2003.
- [61] A. E. Bryson and Y.-C. Ho, Applied Optimal Control: Optimization, Estimation and Control. New York, NY: CRC Press, 1975.
- [62] R. Zou and S. Bhattacharya, "Visibility-based finite-horizon target tracking game," *IEEE Robot. Automat. Lett.*, vol. 1, no. 1, pp. 399–406, Jan. 2016.
- [63] E. A. Coddington and N. Levinson, Theory of Ordinary Differential Equations. New York, NY, USA: McGraw-Hill, 1955.
- [64] I. M. Mitchell, A. M. Bayen, and C. J. Tomlin, "A time-dependent Hamilton-Jacobi formulation of reachable sets for continuous dynamic games," *IEEE Trans. Autom. Control*, vol. 50, no. 7, pp. 947–957, Jul. 2005.
- [65] R. Zou and S. Bhattacharya, "Approximation of capture sets in visibility-based target-tracking games for non-holonomic players," in *Proc. Dyn. Syst. Control Conf.*, 2017, paper DSCC2017-5379.
- [66] B. P. Gerkey and M. J. Matarić, "A formal analysis and taxonomy of task allocation in multi-robot systems," *Int. J. Robot. Res.*, vol. 23, no. 9, pp. 939–954, 2004.
- [67] S. Chopra, G. Notarstefano, M. Rice, and M. Egerstedt, "Distributed version of the Hungarian method for a multirobot assignment," *IEEE Trans. Robot.*, vol. 33, no. 4, pp. 932–947, Aug. 2017.
- [68] R. R. Burridge, A. A. Rizzi, and D. E. Koditschek, "Sequential composition of dynamically dexterous robot behaviors," *Int. J. Robot. Res.*, vol. 18, no. 6, pp. 534–555, 1999.
- [69] D. C. Conner, H. Choset, and A. A. Rizzi, "Flow-through policies for hybrid controller synthesis applied to fully actuated systems," *IEEE Trans. Robot.*, vol. 25, no. 1, pp. 136–146, Feb. 2009.
- [70] C. Belta, V. Isler, and G. J. Pappas, "Discrete abstractions for robot motion planning and control in polygonal environments," *IEEE Trans. Robot.*, vol. 21, no. 5, pp. 864–874, Oct. 2005.
- [71] G. J. Laguna and S. Bhattacharya, "Hybrid system for target tracking in triangulation graphs," in *Proc. IEEE Int. Conf. Robot. Automat.*, 2017, pp. 839–844.



Rui Zou received the B.Eng. degree in mechanical engineering from the Dalian University of Technology, Dalian, China, in 2011, and the Ph.D. degree in mechanical engineering from Iowa State University, Ames, IA, USA, in 2017.

She is currently with The MathWorks, Inc., Natick, MA, USA.



Sourabh Bhattacharya (M'12) received the M.S. degree in electrical engineering, the M.A. degree in applied mathematics, and the Ph.D. degree in electrical and computer engineering from the University of Illinois at Urbana–Champaign (UIUC), Champaign, IL, USA, 2005, 2009, and 2012, respectively.

After a Postdoctoral position with Coordinated Science Laboratory, UIUC, he joined the faculty of Iowa State University in 2012, where he is currently with the Departments of Computer Science and Mechanical Engineering. His research interests

include control and motion planning for multirobot systems with adversarial interactions.